Volume 28
Number 8
25 February 2026
Pages 4977–5590

PCCP

Physical Chemistry Chemical Physics

rsc.li/pccp

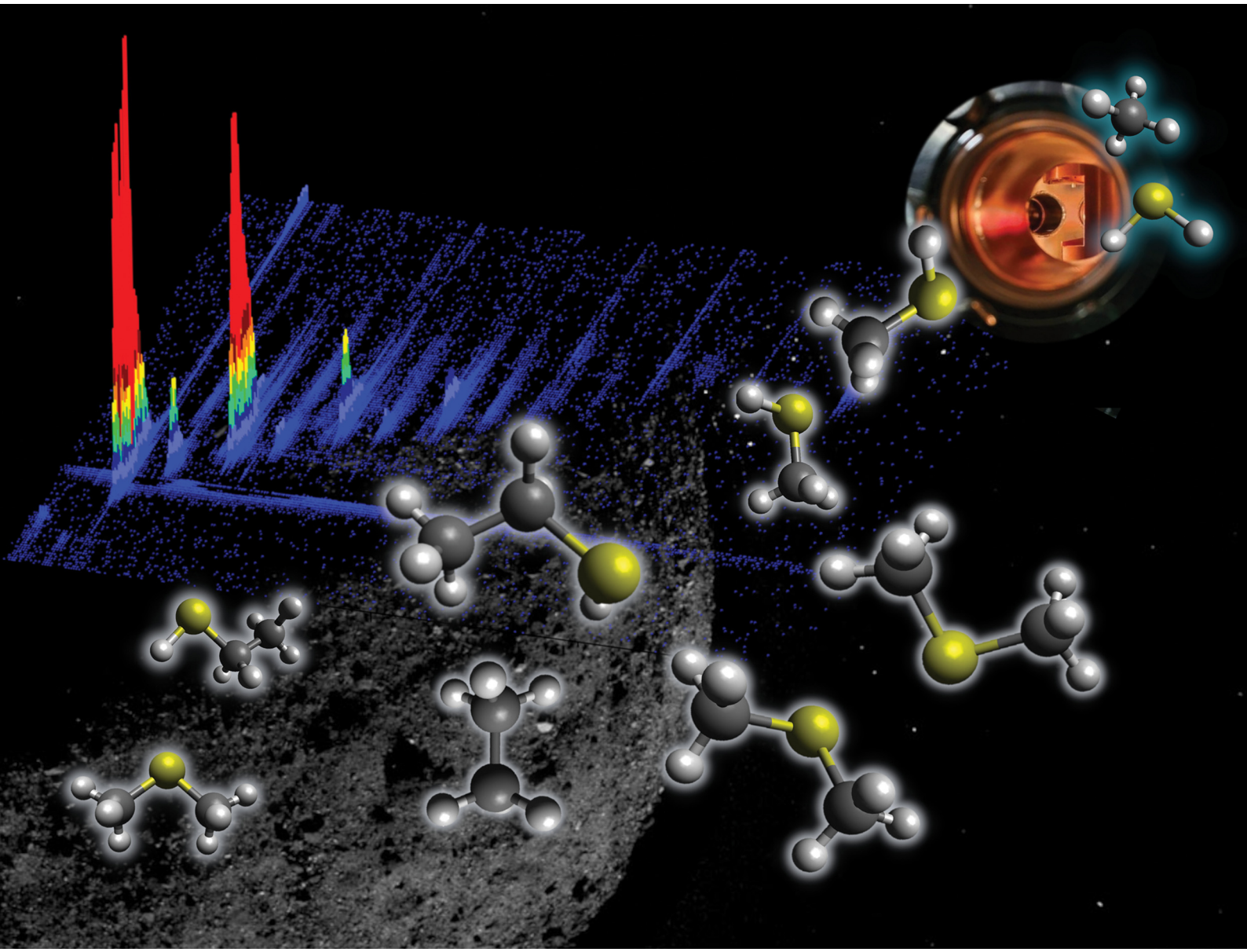

ISSN 1463-9076

ROYAL SOCIETY OF CHEMISTRY

PAPER

Ralf I. Kaiser *et al.*

Formation of dimethyl sulfide (CH_3SCH_3) and ethanethiol (CH_3CH_2SH) in interstellar analog ices of methane (CH_4) and hydrogen sulfide (H_2S)

PCCP Owner Societies

PCCP

ROYAL SOCIETY OF CHEMISTRY

PAPER

View Article Online
View Journal | View Issue

Cite this: *Phys. Chem. Chem. Phys.*, 2026, **28**, 5094

Formation of dimethyl sulfide (CH_3SCH_3) and ethanethiol (CH_3CH_2SH) in interstellar analog ices of methane (CH_4) and hydrogen sulfide (H_2S)

Ashanie Herath, [ab] Andrew M. Turner,[ab] Mason McAnally, [ab] Jia Wang [ab] and Ralf I. Kaiser *[ab]

Received 18th November 2025,
Accepted 16th January 2026

DOI: 10.1039/d5cp04456a

rsc.li/pccp

Hitherto unidentified abiotic formation pathways leading to the organosulfur molecules ethanethiol (C_2H_5SH), methanethiol (CH_3SH) and, dimethyl sulfide (CH_3SCH_3) were investigated through a series of laboratory simulation experiments. Interstellar analog ices of methane (CH_4) and hydrogen sulfide (H_2S) were exposed to proxies of galactic cosmic rays (GCRs) in the form of energetic electrons released in the GCR track in interstellar ices simulating typical cold molecular cloud lifetimes of a few 10^6 to 10^7 years. During the temperature-programmed desorption phase, the molecules subliming fractionally from the ice mixtures were photoionized with vacuum ultraviolet (VUV) photons at energies both above and below the adiabatic ionization energies of the product molecules of interest. Exploiting photoionization reflectron time-of-flight mass spectrometry (PI-ReToF-MS) and isotopically labelled ice experiments, the reaction products were selectively photoionized to discriminate between isomers. Ethane (C_2H_6) and methanethiol (CH_3SH), as first-generation irradiation products, along with second-generation dimethyl sulfide (CH_3SCH_3), were identified *via* infrared spectroscopy and PI-ReToF-MS. The formation of ethanethiol (C_2H_5SH) was further confirmed by matching the photoionization efficiency (PIE) curve to the experimental PI-ReToF-MS data. Our findings instigate a deeper understanding of interstellar sulfur chemistry linking interstellar and cometary ices to the gas-phase detection of sulfur bearing organics in star-forming regions.

Introduction

In the search of carbonaceous life as we know it on extraterrestrial planets, terrestrial molecules of sole biotic origins are exploited as biosignatures.[1,2] Dimethyl sulfide (CH_3SCH_3), dimethyl disulfide (CH_3SSCH_3), and methanethiol (CH_3SH) have been discussed as such biomarkers and organosulfur compounds of early Earth-like biospheres[2–4] based on their functional and/or chemical characteristics derived from biological entities in extraterrestrial rocky or aquatic planetary environments.[5,6] A recent investigation of the exoplanet K2-18 b, located 120 light years away from Earth, reported a possible detection of dimethyl sulfide (CH_3SCH_3) utilizing the James Webb space telescope (JWST) near-infrared spectrograph (NIRSpec) and near-infrared imager and slitless spectrograph (NIRISS).[7] However, the observations of these molecules in the interstellar medium (ISM) and in comets have challenged the designation of those sulfur-bearing molecules as biomarkers considering plausible, but hitherto unknown abiotic formation routes in deep space. Furthermore, the interstellar detection of thiols (RSH), with R being an alkyl chain,[8–10] like methanethiol (CH_3SH) and ethanethiol (C_2H_5SH) suggest the extraterrestrial formation of these molecules and their subsequent delivery to early Earth and other Earth-like biospheres.

As one of the simplest sulfur-bearing complex organic molecules (COMs), methanethiol (CH_3SH), also known as methyl mercaptan, was first observed toward the Sagittarius B2 molecular cloud[11] and in multiple other star-forming regions such as the hot cores Orion KL and G327.3-0.6.[12,13] Singly deuterated methyl mercaptan (CH_2DSH) was detected toward the protostar IRAS 16293-2422 B.[14] Ethyl mercaptan, also known as ethanethiol (C_2H_5SH), was tentatively assigned toward Orion KL[12] and later confirmed toward the galactic center quiescent cloud G+0.693–0.027.[10] The structural isomer of ethanethiol, dimethyl sulfide (CH_3SCH_3), was recently observed toward G+0.693–0.027 as well.[15] In addition to the detections of these molecules in the interstellar medium, ionized methanethiol (CH_3SH; mass-to-charge ratio (m/z) = 48), and ethanethiol and/or dimethyl sulfide (C_2H_6S; m/z = 62) were

[a] *Department of Chemistry, University of Hawai'i at Mānoa, Honolulu, HI 96822, USA. E-mail: ralfk@hawaii.edu*
[b] *W. M. Keck Laboratory in Astrochemistry, University of Hawai'i at Mānoa, Honolulu, HI 96822, USA*

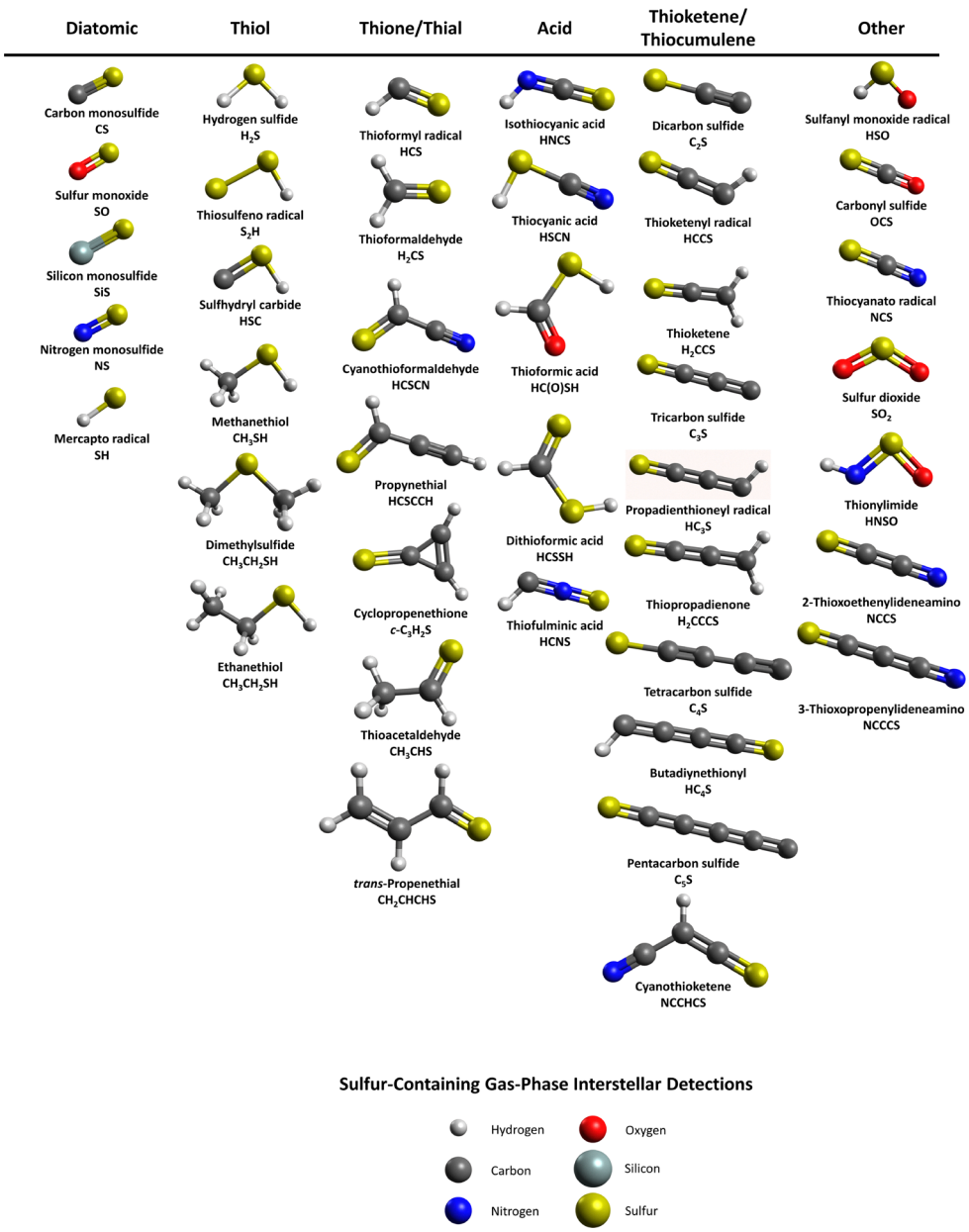

Fig. 1 Up-to-date inventory of neutral sulfur containing molecules identified in the interstellar environments. The atom colors are of the following correspondence. Hydrogen: white, carbon: grey, nitrogen: blue, oxygen: red, silicon: teal and sulfur: yellow.

identified in the coma of comet 67P/Churyumov–Gerasimenko with the double focusing mass spectrometer (DFMS) of Rosetta orbiter spectrometer for ion and neutral analysis (ROSINA) instrument onboard the Rosetta mission, with hydrogen sulfide (H_2S) being the dominant sulfur species in the coma.[16,17] The carrier of the signal at m/z = 62 remained elusive until Hänni *et al.* revisited the electron ionization fragmentation patterns of both ethanethiol and dimethyl sulfide, thus identifying the carrier of m/z = 62 as dimethyl sulfide.[18] Furthermore, organosulfur molecules of $C_nH_mS_p$ (n = 0–4, m = 0–6, and p = 1, 2) have been identified in the cometary coma 67P/CG as well.[19]

With the observational confirmation of dimethyl sulfide, along with forty neutral organosulfur molecules in extraterrestrial environments (Fig. 1), attention has been devoted to the elucidation of the formation pathways of these sulfuretted molecules. Previous laboratory experiments have incorporated sulfur-containing ices such as hydrogen sulfide (H_2S) or sulfur dioxide (SO_2),[19–30] and sulfur atom bombardments[31,32] to probe the astrophysically relevant sulfur chemistry. On these interstellar analog ices, sulfanes (H_2S_n), sulfur allotropes,[20,22,24,33] and organosulfur molecules as complex as thioacids[26] and alkylsulfonic acids have been reported.[30] Gas phase photochemical experiments with hydrogen sulfide (H_2S) containing gas mixtures of carbon dioxide (CO_2) and methane (CH_4) probing the atmosphere of planet K2-18b observed the abiotic formation of dimethyl sulfide as an

alternative abiotic formation route on planetary bodies with pronounced volcanic activity.[34]

Here, laboratory simulation experiments were conducted at the W. M. Keck Research Laboratory in Astrochemistry exploiting the effects of proxies of galactic cosmic rays (GCRs) on interstellar ices composed of hydrogen sulfide (H_2S) and the simplest alkane, methane (CH_4). Ices were processed at low temperatures of 5 K with energetic electrons to mimic the interaction of secondary electrons that are generated in the tracks of galactic cosmic rays that penetrate the icy interstellar dust grains over a typical cold molecular cloud lifetime of a few 10^6 to 10^7 years.[35–37] Fourier transform infrared spectroscopy (FTIR) was utilized to characterize the deposited and processed ices. Tunable vacuum ultraviolet (VUV) photoionization reflectron time-of-flight mass spectrometry (PI-ReToF-MS)[35,38] enabled isomer-specific identification of molecules in the gas phase as they sublimed from the icy frost during temperature programed desorption (TPD) phase of the ice mixtures. This phase simulates the post-gravitational collapse stage and the inherent gradual warm up of the neighboring environments of dust grains. These studies present the first laboratory evidence for the abiotic formation of dimethyl sulfide (CH_3SCH_3) and ethanethiol (C_2H_5SH) in interstellar analog ices exploiting modern, isomer-selective photoionization techniques. At m/z = 62, the dimethyl sulfide isomer (CH_3SCH_3) was confirmed *via* PI-ReToF-MS, while ethanethiol CH_3CH_2SH) was identified through the analysis of the photoionization efficiency (PIE) curve. Furthermore, formation pathways were investigated utilizing partially deuterated ices of methane–hydrogen sulfide (CD_4–H_2S) and deuterium sulfide–methane (CH_4–D_2S). Our findings are crucial for linking the detection of methyl- and ethyl thiol along with dimethyl sulfide in the interstellar medium,[10,11,15] in comet 67P/CG,[16,18] and potentially on exoplanet K2-18 b,[7] to a viable abiotic formation route in the solid state.

Experimental section

The experiments were conducted in a hydrocarbon-free stainless steel ultrahigh-vacuum chamber at pressures of a few 10^{-11} Torr generated by two magnetically suspended turbomolecular pumps in series (Osaka, TG420MCAB and TG1300MUCWB) and backed by an oil free scroll pump (Edwards, GVSP30). In the chamber, a highly-polished silver wafer is placed on a freely-rotatable cold-finger, which can be cooled down to 5.2 ± 0.2 K using a two-stage, closed-cycle helium compressor (Sumimoto Heavy Industries, RDK-415E) as described previously.[38,39] A premixed hydrogen sulfide (H_2S, Sigma Aldrich, ≥99.5%) and methane (CH_4, Airgas, >99.9%) gas mixture of H_2S–CH_4 at a 3 : 7 gas-phase ratio was introduced into the main chamber *via* a glass capillary array and condensed on the silver wafer at a pressure of 4×10^{-8} Torr. The ice deposition on the silver wafer was monitored *in situ* using a He–Ne laser (MellesGriot, 25-LHP-230, 632.8 nm). Employing refractive index (n) of 1.41 for hydrogen sulfide and 1.34 for methane, the thickness of the ices was calculated to be 1100 ± 200 nm with an average refractive index of 1.37 ± 0.05 for the mixed ice.[40–42] To simulate the secondary electrons formed in the track of GCRs penetrating the ices, each deposited ice was processed with 5 keV energetic electrons isothermally at 5 K. Two irradiation doses were used for the two main goals of the experiment. First, a high irradiation dose of 60 minutes at 1000 nA, was used to identify the irradiation products formed in these ices, and secondly, a low dose of 10 minutes at 10 nA, was used to identify the isomeric mass shifts in retrosynthetic pathways *via* intermediate identifications (Table 1). Energetic electrons were generated *via* an electron gun (Specs PU-EQ 22). The average penetration depth of the electrons was found to be 400 ± 50 nm using CASINO simulations.[43] Ices were deposited thicker than the simulated penetration depth to eliminate reactions at the interface of the ice and the silver substrate. The ratios of the deposited ices of methane and hydrogen sulfide were determined utilizing the IR bands and band absorption coefficients of fundamentals ν_1/ν_3 (H_2S, 1.12×10^{-17} cm molecule^{-1}), ν_4 (CH_4, 1.3×10^{-18} cm molecule^{-1}), combination bands $\nu_1 + \nu_4$ (CH_4, 2.9×10^{-19} cm molecule^{-1}), and $\nu_3 + \nu_4$ (CH_4, 4.2×10^{-19} cm molecule^{-1}) (Table 1).[40,42] A Fourier transform infrared spectrometer (FTIR, Nicolet 6700) with a mercury–cadmium–telluride (Thermo, MCT-B) detector was used in the range of 6000–500 cm^{-1} and a spectral resolution of 4 cm^{-1} to monitor the chemical changes of the deposited ices *in situ* after deposition and

Table 1 Parameters and dosage calculations of methane–hydrogen sulfide ices

Irradiated area (cm^2)	1.6 ± 0.1			
Initial kinetic energy (keV)	5.0			
Average energy of transmitted electrons (keV)	0.0			
Irradiation current (nA)	10 ± 1			100 ± 11
Total number of electrons	(3.74 ± 0.06) × 10^{13}			(2.25 ± 0.04) × 10^{15}
Fraction of transmitted electrons	0.0			0.0
	Low dose, at 10.49 eV			High dose, at 9.34 eV, 8.75 eV, and 8.17 eV
Ice composition	CH_4–H_2S	CD_4–H_2S	CH_4–D_2S	CH_4–H_2S
Ratio	0.2 ± 0.1 : 1	0.2 ± 0.1 : 1	0.4 ± 0.2 : 1	0.2 ± 0.1 : 1
Density of mixed ice (g cm^{-1})	0.561	0.621	0.543	0.561
Average thickness (nm)	1570 ± 200			1100 ± 200
Average penetration depth (nm)	400 ± 50			400 ± 50
Dose per molecule of methane (eV molecule^{-1})	0.12 ± 0.04	0.12 ± 0.04	0.16 ± 0.04	7.3 ± 0.3
Dose per molecule of hydrogen sulfide (eV molecule^{-1})	0.27 ± 0.04	0.26 ± 0.04	0.28 ± 0.04	15.6 ± 0.3

irradiation. After the irradiation, the ices were warmed up from 5 to 330 K exploiting temperature–programmed desorption (TPD) at rate of 1 K min^{-1} with the help of a temperature programmable controller (Lake Shore 336) simulating the transformation of cold molecular clouds to star-forming regions.

During TPD, molecules subliming to the gas phase were analyzed *via* tunable, single photon ionization exploiting pulsed (30 Hz) vacuum ultraviolet (VUV) light. VUV photons at energies 10.49, 9.34, 8.75, and 8.17 eV were generated *via* resonant or non-resonant four-wave mixing (FWM) of two pulsed laser beams overlapped in space and time with xenon (99.999%) or krypton (99.999%) as non-linear medium (Fig. 2). A reflectron time-of-flight (ReToF) mass spectrometer (Jordan TOF Products, Inc.) analyzed the photoionized species isomer-specifically. The third harmonic of a pulsed neodymium yttrium-aluminum garnet (Nd:YAG, Spectra-Physics, Quanta Ray PRO 250-30) laser was utilized to generate the 10.49 eV photons *via* frequency tripling in xenon. The third harmonic of a second pulsed Nd:YAG laser (Spectra-Physics, Quanta Ray PRO 270-30) was used to pump a dye laser (Sirah Lasertechnik, Cobra-Stretch) containing Stilbene-420 dye to obtain 425.112 nm, which undergoes second harmonic generation to produce 212.556 nm (ω_1). Coherent VUV light of 9.34 eV energy was generated by spatially overlapping and time synchronizing colinear beams of ω_1 (212.556 nm) with the third harmonic of the other pulsed Nd:YAG laser (ω_2 = 355 nm) in an evacuated chamber with pulsed jets of krypton gas (30 Hz). Likewise, in generating other wavelengths listed in Table 2, four-wave mixing was utilized with the corresponding dye solutions indicated. The VUV light of relevant energy was spatially separated from interfering wavelengths utilizing a biconvex lithium fluoride lens (ISP Optics) positioned off axis to the beam. The VUV beam of desired energy was passed through a 1 mm aperture, 2.0 ± 0.5 mm above the substrate surface, to photoionize the subliming molecules during TPD. The resulting ion signals were collected by a reflectron time-of-flight mass spectrometer (ReToF-MS; Jordan TOF Products, Inc.) and detected by microchannel plate (MCP) detector. A preamplifier (Ortec 9305) was incorporated to amplify the signal. The signal arriving in 4 ns bin width times were analyzed with a multichannel scaler (FAST ComTec, MCS6A).[44] The integration of mass spectra of 3600 sweeps at 30 Hz corresponds to an integration time of 2 minutes.

Photon energies were chosen to distinguish between the adiabatic ionization energies (IEs) of methanethiol (**1**, CH_3SH), dimethyl sulfide (**2**, CH_3SCH_3), and ethanethiol (**3**, CH_3CH_2SH). The IEs of these molecules are well known from the literature. The IEs of methanethiol, ethanethiol, and dimethyl sulfide are reported as 9.439 ± 0.005 eV,[45] 9.31 ± 0.03 eV,[45] and 8.69 ± 0.02 eV,[45] respectively. The observable IEs indicated in Fig. 2 include the errors and corrected for the Stark effect of the ReToF acceleration field by −0.03 eV (Table 3). Only VUV photons with energies above the ionization threshold of a given molecule can produce the corresponding molecular ion; the resulting radical cation may undergo dissociation in the gas phase at above their threshold for dissociative photoionization.[46] In principle, molecules undergoing dissociative photoionization may contribute ion signal at corresponding fragment masses as they sublime; this can be evidenced or disproven by, *e.g.*, comparing the TPD profiles of the parents with the fragments. At 10.49 eV, all the three molecules if present can be ionized, whereas 9.34 eV photons can ionize both isomers dimethyl sulfide (**2**) and ethanethiol (**3**) at m/z = 62, but not methanethiol (**1**) at m/z = 48. VUV photons of 8.75 eV can aid in differentiating between the two isomers at m/z = 62 and can only ionize dimethyl sulfide (**2**). The experiment carried out at 8.17 eV photon energy is below the ionization energies of all three molecules of interest. The photon energies of 8.75 eV and 9.34 eV employed in the experiments are close to the ionization energies of dimethyl sulfide (**2**, IE = 8.69 ± 0.02 eV) and ethanethiol (**3**, IE = 9.31 ± 0.03 eV), respectively, thereby excluding the fragmentation of isomers **2** and **3** upon photoionization. An additional experiment with no irradiation (blank) photoionizing with 10.49 eV photons was conducted to confirm that no thermal reactions caused the formation of

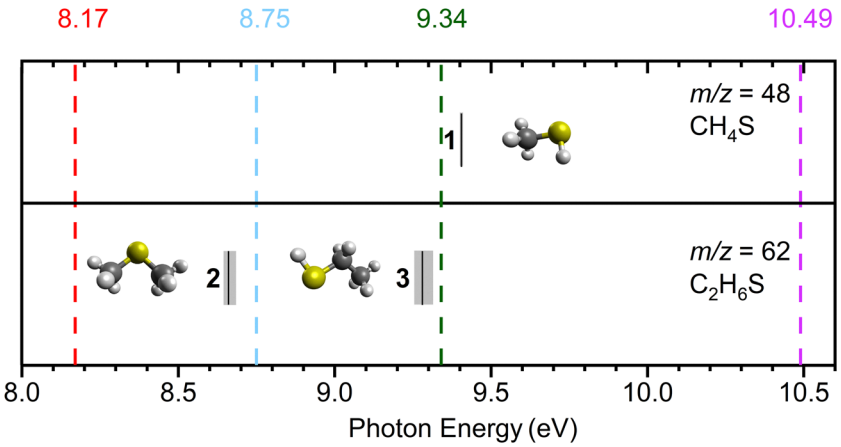

Fig. 2 Ranges of adiabatic ionization energies of methanethiol (CH_3SH, **1**), dimethyl sulfide (CH_3SCH_3, **2**) and its isomer ethanethiol (C_2H_5SH, **3**) incorporating thermal and stark effect are denoted in grey, while the black lines indicate their measured ionization energies. Colored dashed lines indicate the different photoionization energies at which the experiments were conducted to collect ReToF-MS data.

Table 2 Photoionization experiments utilize four-wave mixing schemes to generate vacuum ultraviolet (VUV) photons. At least one dye laser pumped by a Nd:YAG laser was used with appropriate harmonic (355 or 532 nm) in accordance with the dye

Medium	ω_{VUV}	Nd:YAG wavelength (nm)	ω_1 (nm)	ω_1 dye	Nd:YAG wavelength (nm)	ω_2 (nm)	ω_2 dye	Energy (eV)
Xenon	$3\omega_1$	355[a]	—	—	—	—	—	10.49
Krypton	$2\omega_1 - \omega_2$	355	212.556	Stilbene 420	532	532[a]	—	9.34
Krypton	$2\omega_1 - \omega_2$	355	212.556	Stilbene 420	—	425.112	—	8.75
Krypton	$2\omega_1 - \omega_2$	355	212.556	Stilbene 420	355	355[a]	—	8.17

[a] Nd:YAG harmonic.

Table 3 Error analysis of adiabatic ionization energies (IEs) of methanethiol (**1**), dimethyl sulfide (**2**), and ethanethiol (**3**). The observable IE ranges are obtained *via* correcting for the thermal and Stark effects by −0.03 eV

	Molecule/isomer	*m*/*z*	Structure	IE (evaluated per eV)	IE range with error (eV)	Corrected IE with Stark effect (eV)
1	CH_3SH	48	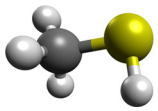	9.439 ± 0.005[45]	9.434–9.444	9.40–9.41
2	CH_3SCH_3	62	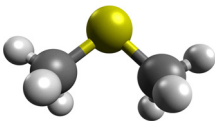	8.69 ± 0.02[45]	8.67–8.71	8.64–8.68
3	C_2H_5SH	62	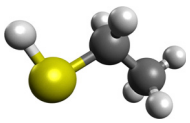	9.31 ± 0.03[45]	9.28–9.34	9.25–9.31

products. Isotopically labeled ice mixtures CH_4–D_2S (D_2S, Sigma Aldrich, 97 atom % D, Fig. S1), and CD_4–H_2S (CD_4, Sigma-Aldrich, 99.9 atom % D, Fig. S2) were compared to product masses observed on CH_4–H_2S ice processed with a low irradiation dose at 10.49 eV, to confirm the assignments and the formation pathways.

Results and discussion

Infrared spectroscopy

Fourier transform infrared (FTIR) spectroscopy was used to characterize the deposited ices. All absorption features observed in pristine ices were associated with fundamentals or overtone bands of hydrogen sulfide and methane (Fig. 3A). A combination of symmetric and antisymmetric stretching modes of S–H bonds (ν_1 and ν_3) gave a strong characteristic peak for hydrogen sulfide in the range of 2581–2560 cm^{-1}. The bending mode of H_2S (ν_2) emerges as a peak of weak intensity at 1169 cm^{-1}.[47,48] Methane displayed the fundamentals ν_3 (3010–3003 cm^{-1}), ν_4 (1300–1295 cm^{-1}), and a small peak for infrared inactive ν_2 (1528 cm^{-1}) vibration.[42,49] After the irradiation, new infrared (IR) absorption features were observed and deconvoluted in cyan in Fig. 3B. A difference IR spectrum was obtained between after and before irradiation is included in Fig. 3C. Table 4 summarizes the IR absorption features of the deposited pristine ices compared to the features after irradiation.

Ethane (C_2H_6) was identified *via* its fundamentals ν_1 (2974 cm^{-1}), ν_{10} (2960 cm^{-1}), ν_5 (2881 cm^{-1}), ν_{11} (1462 cm^{-1})[49] and $\nu_8 + \nu_{11}$ overtone at 2939 cm^{-1}. Absorption feature adjacent to ν_{11} (C_2H_6, 1462 cm^{-1}), at 1437 cm^{-1} is assigned to scissoring CH_2 vibrations (ν_{12}) of C_2H_4.[49] Broadening of S–H stretching was observed in 2495 cm^{-1} due to the formation of disulfane (ν_5, H_2S_2) and other higher order sulfanes (H_2S_n; $n > 2$).[22,24,50] Carbon disulfide (CS_2) was identified by its strongest absorption feature, ν_3, at 1513 cm^{-1}.[51] In the range 1460–1400 cm^{-1}, methyl residues connected to sulfur atoms (–SCH_3) show symmetric CH_3 deformation vibration features and in the range 1435–1410 cm^{-1}, CH_2 deformation vibrations by –CH_2–S– moieties.[52] Thus, the features observed at 1429 and 1414 cm^{-1} are assigned to these deformation vibrations. Since FTIR limits the identifications to functional groups in case of complex icy mixtures, an alternative isomer specific technique is required to investigate the individual products formed.

Photoionization reflectron time-of-flight mass spectrometry (PI-ReToF-MS)

Tunable vacuum-ultraviolet (VUV) photoionization coupled with reflectron time-of-flight mass spectrometry (PI-ReToF-MS) was utilized to identify the molecules sublimed into the gas phase during TPD. PI-ReToF-MS provides a unique approach in an isomer-selective detection with soft photoionization of molecules of interest *via* selection of photon energies that would not fragment the molecular parent ions, unlike in electron impact (EI) mass detections with fixed electron

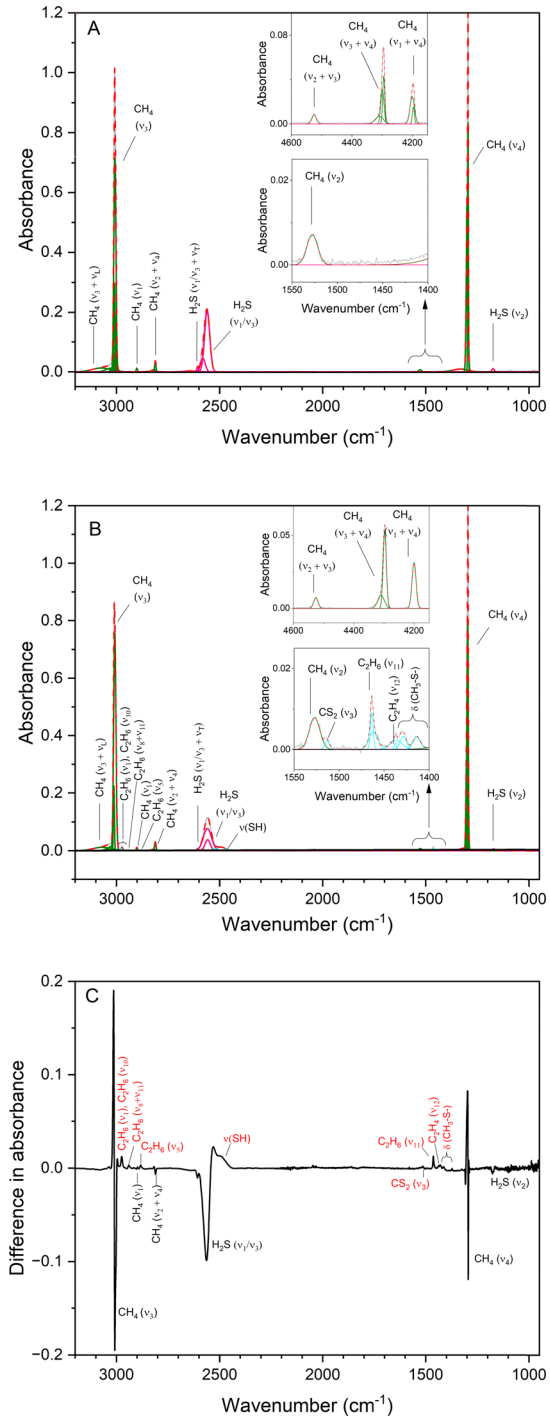

Fig. 3 Infrared spectra of methane (CH_4) and hydrogen sulfide (H_2S) ice. Original spectrum (grey) is deconvoluted showing the peaks assigned to hydrogen sulfide (pink) and methane (green). The red dashed line is the sum of deconvoluted Gaussian peaks. (A) Pristine ice at 5 K. (B) New features emerged after irradiation are indicated in cyan (Table 4). Insets include the magnified regions 4600–4150 cm^{-1} and 1550–1400 cm^{-1}. (C) A difference IR spectrum was obtained between after and before irradiation. A blue shift is observed in the reactant peaks. The new IR features observed after irradiation are indicated in red.

Table 4 Infrared absorption assignments of methane (CH_4) and hydrogen sulfide (H_2S) ices before irradiation and the products formed after electron irradiation

Assignment		Position (cm^{-1})	Ref.
Before irradiation CH_4–H_2S ice (10 K)			
$\nu_2 + \nu_3$	CH_4	4525	49
$\nu_3 + \nu_4$	CH_4	4309, 4299, 4295	49
$\nu_1 + \nu_4$	CH_4	4201, 4197	49
$\nu_3 + \nu_L$	CH_4	3074, 3028	49
ν_3	CH_4	3010, 3008, 3003	49
ν_1	CH_4	2902	49
$\nu_2 + \nu_4$	CH_4	2837, 2818, 2812	49
$\nu_1/\nu_3 + \nu_R$	H_2S	2644	47
$\nu_1/\nu_3 + \nu_T$	H_2S	2607	47
ν_1/ν_3	H_2S	2581, 2560	47
ν_2	CH_4	1528	49
$\nu_4 + \nu_L$	CH_4	1334	42
ν_4	CH_4	1300, 1295	49
ν_2	H_2S	1174	47
Before irradiation CH_4–D_2S ice (10 K)			
$\nu_2 + \nu_3$	CH_4	4525	49
$\nu_3 + \nu_4$	CH_4	4312, 4300, 4295	49
$\nu_1 + \nu_4$	CH_4	4199	49
$\nu_3 + \nu_L$	CH_4	3083, 3025	49
ν_3	CH_4	3010, 3007, 3003	49
ν_1	CH_4	2901	49
$\nu_2 + \nu_4$	CH_4	2820, 2812	49
$\nu_1/\nu_3 + \nu_2$	D_2S	2733, 2709	47
$\nu_1/\nu_3 + \nu_T$	H_2S	2602	47
ν_1/ν_3	H_2S	2590, 2560	47
$\nu_1/\nu_3 + \nu_R$	D_2S	1945	47
$\nu_1/\nu_3 + \nu_T$	D_2S	1893	47
ν_1/ν_3	D_2S	1873, 1855	47
ν_2	CH_4	1528	49
$\nu_4 + \nu_L$	CH_4	1361, 1325	42
ν_4	CH_4	1300, 1296	49
ν_2	D_2S	849	47
Before irradiation CD_4–H_2S ice (10 K)			
$2\nu_3$	CD_4	4474	72
...	...	4308	72
$\nu_3 + 2\nu_4 + \nu_L$	CD_4	4221	72
$\nu_3 + 2\nu_4$	CD_4	4191	72
$\nu_3 + \nu_4$	CD_4	3239, 3234	72
$\nu_1 + \nu_4$	CD_4	3086	72
ν_1	CHD_3	2978	72
$\nu_1/\nu_3 + \nu_R$	H_2S	2653	47
$\nu_1/\nu_3 + \nu_T$	H_2S	2608	47
ν_1/ν_3	H_2S	2579, 2560	47
...	...	2339	72
$\nu_3 + \nu_L$	CD_4	2305	72
ν_3	CD_4	2262, 2254, 2251, 2248, 2236	72
$\nu_2 + \nu_4$	CD_4	2090, 2072	72
$2\nu_4$	CD_4	1980, 1974	72
ν_1/ν_3	D_2S	1879, 1859	47
ν_2	H_2S	1175	47
$\nu_4 + \nu_L$	CD_4	1026	72
ν_4	CD_4	991, 986	72
New features after irradiation CH_4–H_2S ice (10 K)			
ν_1	C_2H_6	2974	49
ν_{10}	C_2H_6	2960	49
$\nu_8 + \nu_{11}$	C_2H_6	2939	49
ν_5	C_2H_6	2881	49
ν(S–H)	H_2S_n ($n > 2$)	2495	24
ν_3	CS_2	1513	51 and 73
ν_{11}	C_2H_6	1464	49
ν_{12}	C_2H_4	1437	49
$\delta(CH_3–S–)$	CH_3–S–/–CH_2S–	1429, 1414	52

energies 70–100 eV.[53,54] A species can only be detected by choosing a photon energy higher than its IE; no parent ion signal is expected with photons of energy below its IE.[39,54] The PI-ReToF-MS data collected during TPD of irradiated and

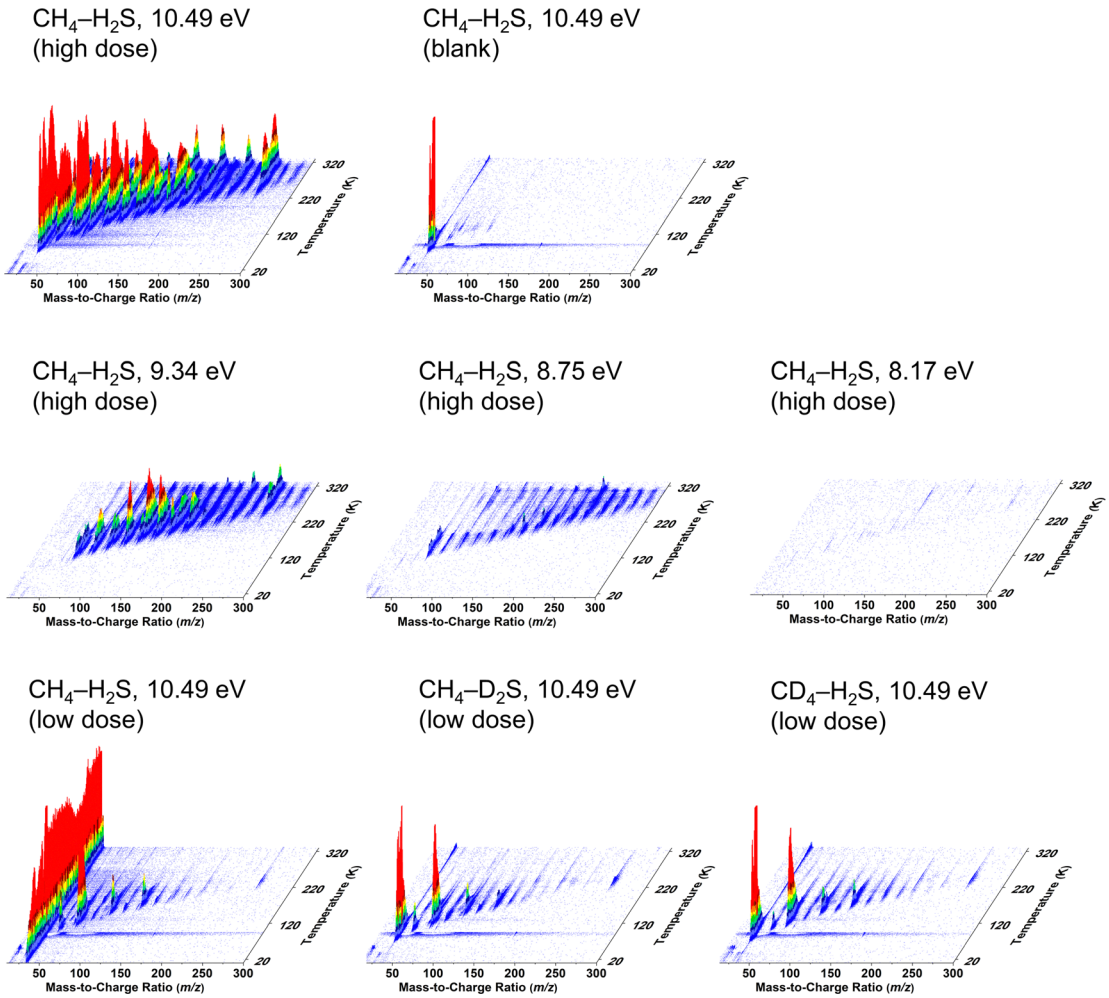

Fig. 4 PI-ReToF-MS data collected during TPD of processed methane–hydrogen sulfide ices. Data were collected for a non-irradiated CH_4–H_2S ice (blank), high irradiation dose processed CH_4–H_2S ices at 10.49 eV, 9.34 eV, 8.75 eV, 8.17 eV, and a low irradiation dose processed CH_4–H_2S, CH_4–D_2S, and CD_4–H_2S ices.

non-irradiated ices of methane and hydrogen sulfide are compiled in Fig. 4. The first sublimation event in both irradiated and non-irradiated (blank experiment) ices photoionized at 10.49 eV is the desorption of hydrogen sulfide with a peak sublimation temperature of 90 K. The H_2S desorption peak is absent in photoionization energies employed below the IE of H_2S, 10.453 ± 0.008 eV.[55] Methane desorption event at 40 K is not recorded *via* mass spectrometry as the ionization energy of methane is higher than the photon energies utilized to ionize the subliming molecules (IE = 12.61 ± 0.01 eV).[56] Only the H_2S sublimation event is observed in the unirradiated CH_4–H_2S ice, confirming all other ion signals observed are a result of energetic electron irradiation on the ices. It should be noted that H_2S trapped amongst the product molecules in the matrix can co–sublime into the gas phase at temperatures higher than 90 K with the gradual sublimation of corresponding molecules (Fig. 4, CH_4–H_2S ice, 10.49 eV, lower irradiation dose). This sublimation behavior may differ in isotopic labeled ices, as previously observed in hydrogen sulfide–carbon monoxide ices.[26] Multiple sublimation events reaching to high molecular masses as high as m/z = 322 are observed with the higher irradiation dose compared to the lower irradiation dose at 10.49 eV. The carriers corresponding to these sublimation events observed were investigated utilizing isotopically labeled experiments. In the irradiated CH_4–H_2S ices, possible species for ion signal of m/z = 62 are C_5H_2, and/or C_2H_6S; for m/z = 48, only C_4 and/or CH_4S have to be considered. Isotopically labeled ices CH_4–D_2S and CD_4–H_2S were used to confirm the molecular formula associated with these mass channels by comparing their TPD profiles and identifying the expected mass shifts resulting from substitution of hydrogen with deuterium as outlined below.

Methanethiol (CH_3SH)

Methanethiol (**1**, CH_3SH, 48 amu) has an adiabatic ionization energy (IE) of 9.439 ± 0.005 eV.[45] Therefore, VUV photons of 10.49 eV were utilized to ionize – if present – methanethiol among the subliming species in the gas phase for CH_4–H_2S ices; photons at 9.34 eV are below the IE of methanethiol and therefore any signal at 10.49 eV should disappear at 9.34 eV for

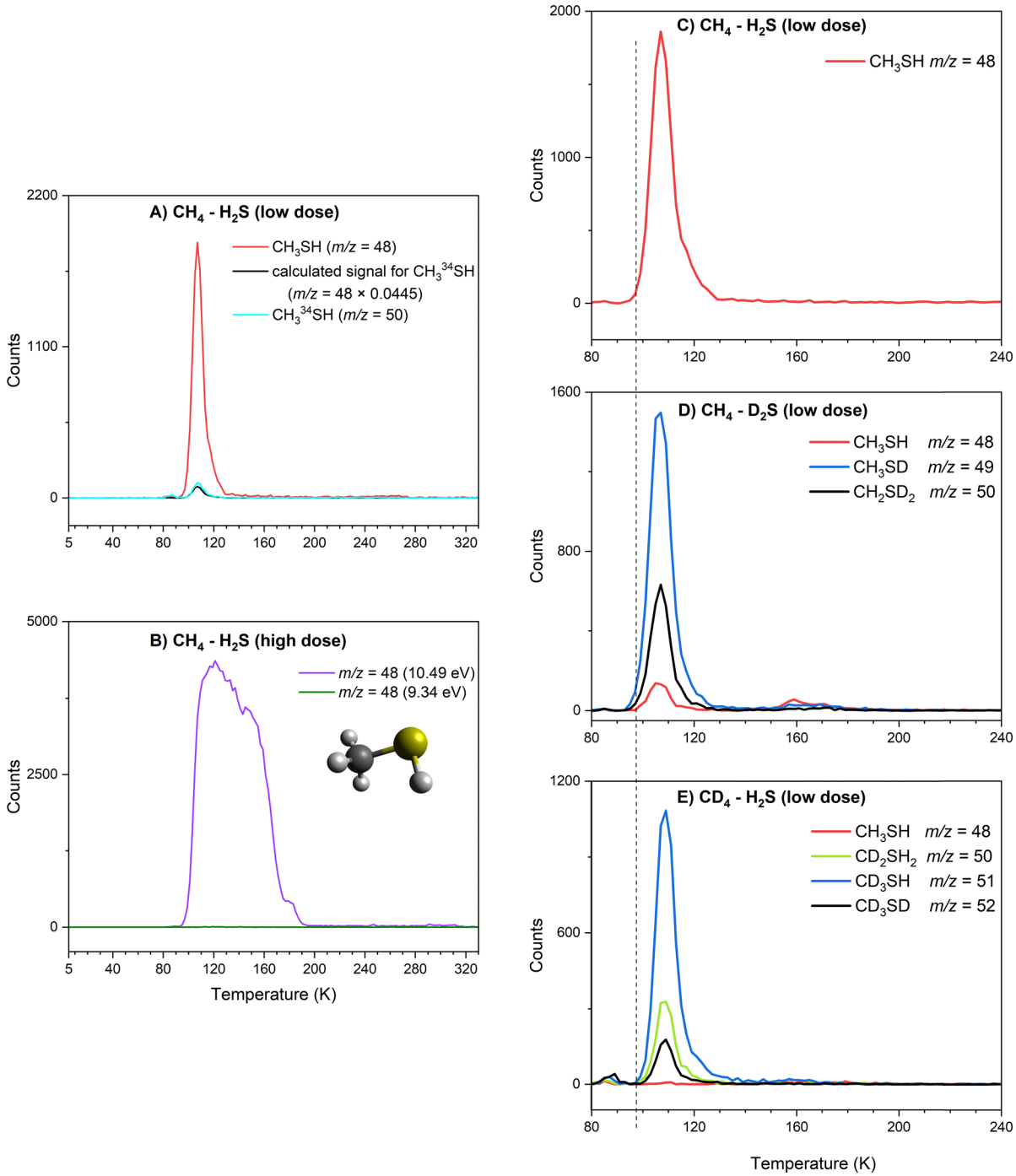

Fig. 5 ReToF-MS data collected for methanethiol identification. (A) Signal at m/z = 48 in the CH_4–H_2S ice photoionized at 10.49 eV during TPD was identified as a single sulfur species by comparing with m/z = 50. (B) TPD profiles of m/z = 48 at 10.49 eV and 9.34 eV in the high irradiation dose experiments. (C)–(E) Comparison of the partially deuterated methanethiol products from the low dose irradiated ices.

m/z = 48. Fig. 5A and Fig. S3 compare the TPD profile recorded at m/z = 48 in the CH_4–H_2S system at 10.49 eV to the signal at m/z = 50, where $CH_3{}^{34}SH$ is expected. The signal for $CH_3{}^{34}SH$ was predicted based on the signal at m/z = 48 and the natural isotopic distribution of sulfur ^{32}S to ^{34}S (4.45%). Overlapping the calculated and the observed signals at m/z = 50 confirms that signal at m/z = 48 belongs to a molecule with a single sulfur atom. In the high dose study, a sublimation peak with an onset at 95 K with an integrated total of 242 730 ± 430 counts, was observed at 10.49 eV, but no ion signal was detected at 9.34 eV (Fig. 5B). Therefore, ion signal of m/z = 48 can be linked to methanethiol (**1**). It should be noted that the broader sublimation event observed at m/z = 48 in the high dose experiment indicates that methanethiol (**1**) was formed in

higher abundance and likely trapped in the ice mixtures and also co-sublime with other irradiation products. To confirm this assignment and its formation mechanisms, low dose irradiation experiments were carried out for partially deuterated ices. Fig. 5C–E compare the sublimation peaks corresponding to (partially) deuterated products of CH_4S in ice mixtures CH_4–H_2S (Fig. 5C), CH_4–D_2S (Fig. 5D), and CD_4–H_2S (Fig. 5E). In the partially deuterated ices, mass shifts up to 4 amu are expected for each deuterium atom replacing hydrogen atoms of CH_4S, where CD_3SD is expected at m/z = 52. In the CH_4–D_2S ice, partially deuterated and/or ^{34}S-labeled methanethiol species observed at m/z = 49 (CH_3SD) and m/z = 50 (CH_2D_2S and $CH_3{}^{34}SH$) are plotted in Fig. 5D, while m/z = 50 (CH_2D_2S and $CH_3{}^{34}SH$), m/z = 51 (CD_3SH and $CH_3{}^{34}SD$), and m/z = 52 (CD_3SD and $CH_2D_2{}^{34}S$) in the irradiated CD_4–H_2S ice are indicated in Fig. 5E. TPD profiles of the isotopically shifted methanethiol species match the sublimation profile of m/z = 48 in the CH_4–H_2S ice (Fig. 5C), indicating that the sublimation peak with an onset at 95 K can be assigned to methanethiol (**1**). It should be noted that the weak sublimation event observed at 90 K is resulted from the saturation of H_2S signal at the detector.

Dimethyl sulfide (CH_3SCH_3)

Above the IEs of C_2H_6S isomers—**2** (dimethyl sulfide, IE = 8.69 ± 0.02 eV) and **3** (ethanethiol, IE = 9.31 ± 0.03 eV)—photon energies of 10.49 eV and 9.34 eV can ionize both isomers if formed (Fig. 2). At 10.49 eV, a sublimation peak at m/z = 62 with an onset of 107 K with a total of 2096 ± 200 counts, was observed in the low-dose irradiated CH_4–H_2S ice (Fig. 6A, peak II). This signal can be attributed to formula(e) C_5H_2 and/or C_2H_6S. The weak sublimation event observed at 90 K is caused by the saturation of the detector upon the sublimation of H_2S (Fig. 6A and B: peak I). At 10.49 eV, signal at m/z = 64 cannot be exploited to check if the signal at m/z = 62 carries a single sulfur atom with natural isotopic distribution of ^{34}S due to the subliming S_2^+ and other fragments. Thus, the mass shifts in the deuterated ice mixtures were investigated to confirm the identity of the signal at m/z = 62. In the low-dose irradiated deuterated ice mixtures of CH_4–D_2S and CD_4–H_2S, ion signals from m/z = 62 to m/z = 68 were investigated (Fig. 6A–C).

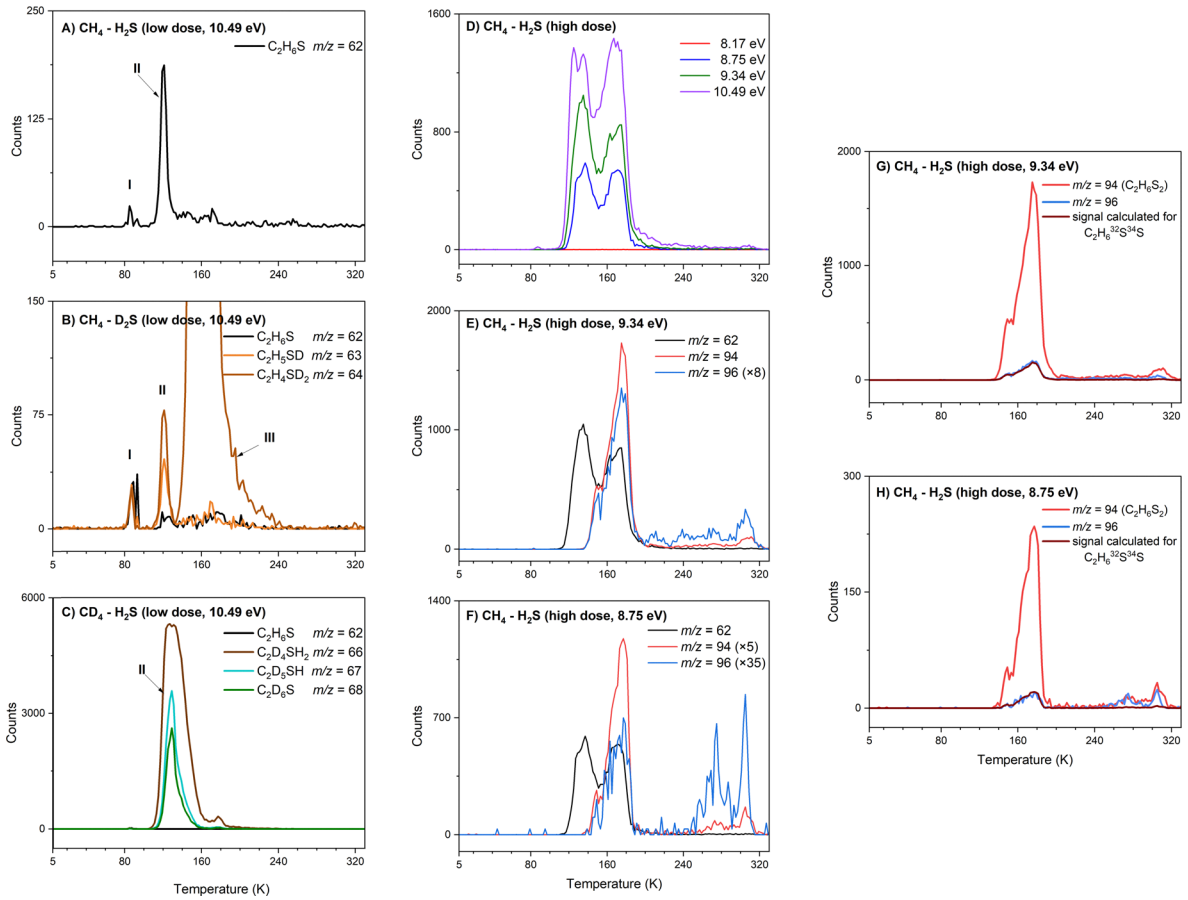

Fig. 6 ReToF-MS data for C_2H_6S isomers photoionized at 10.49 eV during TPD. Panels (A)–(C) depict the ion counts observed for each indicated mass channel in deuterated and non-deuterated ices. Onset sublimation temperature for C_2H_6S isomers were identified as 111 K. (D) TPD profiles of m/z = 62 at 10.49 eV, 9.34 eV, 8.75 eV and 8.17 eV observed two sublimation peaks with the higher irradiation dose. First sublimation peak with an onset at 111 K originated form subliming dimethyl sulfide (CH_3SCH_3), whereas the second sublimation peak observed at m/z = 62 was identified as fragmentation from higher mass channels m/z = 94 and m/z = 96 at both photon energies (B) 9.34 eV and (C) 8.75 eV. Further analysis on the signal at m/z = 94 and m/z = 96 confirms that $C_2H_6S_2$ fragments contribute to the second sublimation peak in m/z = 62 at (G) 9.34 eV and (H) 8.75 eV.

TPD profiles of m/z = 63 and 64 were observed in the CH_4–D_2S ice with an onset sublimation temperature of 109 K, corresponding to C_2H_5SD (m/z = 63), and $C_2H_4SD_2/C_2H_6{}^{34}S$ (m/z = 64) (Fig. 6B). Sublimation event III in Fig. 6B is due to S_2^+ fragment ion, as S_2 (IE = 9.356 ± 0.002 eV)[57] can be photoionized at 10.49 eV. In the irradiated CD_4–H_2S ice, sublimation profiles with an onset of about 110 K were observed at m/z = 66, 67, and 68; these can be linked to partially deuterated products $C_2D_4H_2S$, C_2D_5HS, and C_2D_6S and ^{34}S isotopically labeled molecules $C_2H_4D_2{}^{34}S$, $C_2H_3D_3{}^{34}S$, and $C_2H_2D_4{}^{34}S$ (Fig. 6C). Hence the presence of C_2H_6S isomers at m/z = 62 signal is confirmed.

Having identified the molecular formula for the ions signal at m/z = 62 as C_2H_6S, we are now focusing on elucidating the nature of the isomer formed. TPD profiles of m/z = 62 (C_2H_6S) recorded with photon energies of 10.49 eV, 9.34 eV, 8.75 eV, and 8.17 eV are shown in Fig. 6D at the high irradiation dose. At 10.49 eV and 9.34 eV, at which both isomers **2** and **3** can be ionized, two distinct sublimation peaks were observed with peak sublimation temperatures at 135 K and 171 K. The first peak has an onset at 111 K, similarly to the C_2H_6S peak identified at m/z = 62 in the low dose experiment. The TPD profile recorded at 8.75 eV, which is above the IE of dimethyl sulfide isomer (**2**, IE = 8.64–8.68 eV), but below the IE of ethanethiol (**3**, IE = 9.25–9.31 eV), revealed that two sublimation peaks remain. Lowering the photon energy to 8.17 eV, which cannot ionize dimethyl sulfide (**2**, IE = 8.64–8.68 eV), no sublimation events were detected, indicating that both sublimation peaks are likely associated to **2**. Signal at m/z = 64 was investigated at multiple photon energies to explore potential signal from naturally occurring sulfur isotopes incorporated in $C_2H_6{}^{34}S$ molecules (Fig. 7). At 10.49 eV, only the onset of m/z = 64 signal matches with the expected signal for $C_2H_6{}^{34}S$ ions. But at photon energies 9.34 eV and 8.75 eV, *i.e.* below the IE of S_2 (9.356 ± 0.002 eV),[57] observed signal at m/z = 64 matches the predicted signal for $C_2H_6{}^{34}S^+$ ions, thus confirming the presence of a single sulfur species in both sublimation peaks (Fig. 7). Notably, the second sublimation peak (171 K) overlaps with TPD profiles of m/z = 94 and m/z = 96 suggesting that this signal may originate from fragmentation of ions associated with m/z = 94 and 96 (Fig. 6E and F). Signal at m/z = 96 was found to be 8.9% of m/z = 94, confirming a two-sulfur system at both 9.34 eV (Fig. 6G) and 8.75 eV (Fig. 6H). Therefore, only the first sublimation event with an onset temperature of 111 K can be clearly assigned to dimethyl sulfide (**2**).

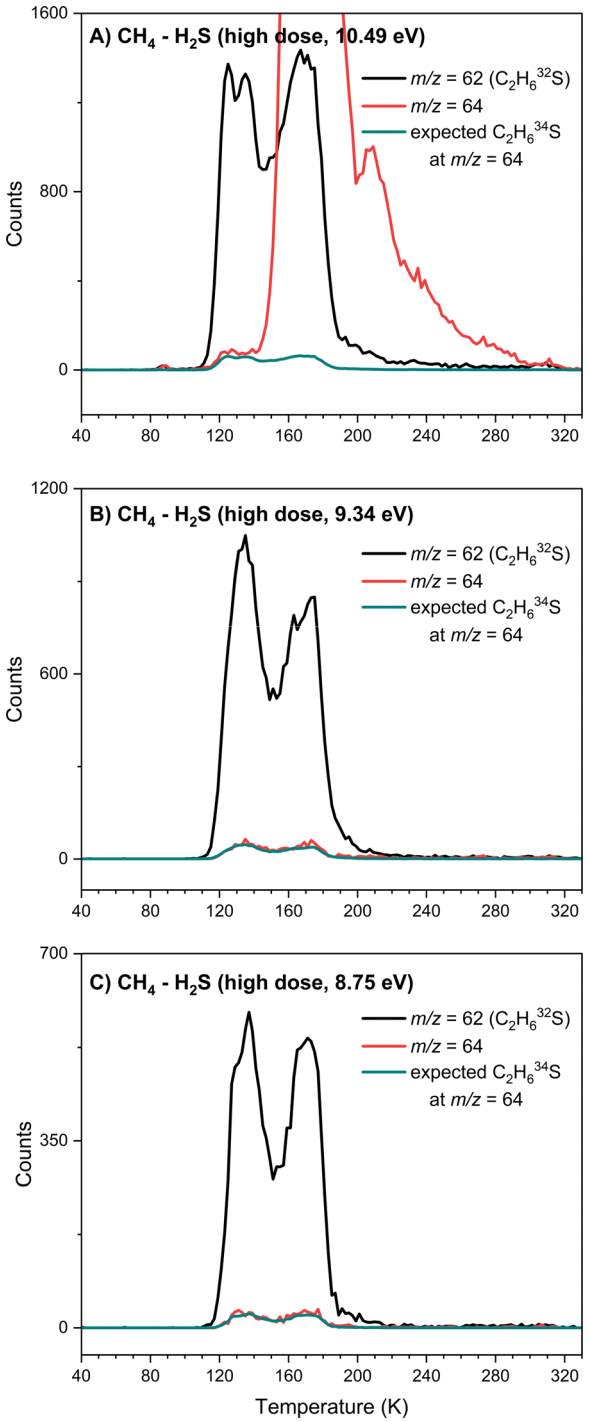

Fig. 7 Signal observed at m/z = 62 and m/z = 64 were used to confirm the assignment C_2H_6S. The expected signal for $C_2H_6{}^{34}S$ (calculated using the signal at m/z = 62), was compared with the signal observed at m/z = 64. (A) At 10.49 eV, the mass channel m/z = 64 comprises of contributions from other ions, whereas at (B) 9.34 eV and (C) 8.75 eV, the observed signal at m/z = 64 is identified as $C_2H_6{}^{34}S$.

Ethanethiol (CH_3CH_2SH)

The PI-ReToF-MS data confirmed the presence of dimethyl sulfide (**2**) among the sublimed gas-phase products at 111 K, whereas ethanethiol (**3**) could not be unambiguously identified based on the ionization energies alone. However, it is possible that ethanethiol (**3**) forms in the irradiated ices and co-sublimes at the same temperature as dimethyl sulfide (**2**). But the contribution of **3** – if any – cannot be quantified *via* PI-ReToF-MS data alone. Therefore, as an additional analytical technique, the photoionization efficiency (PIE) curve, which depicts the relationship between the ion counts at m/z = 62 and the photon energy, was utilized to infer contribution of **3**. PIE curves for both **2** and **3** were obtained from their photoelectron (PE) spectra (Fig. 8).[58,59] This plot can account for 50 ± 25% contribution of dimethyl sulfide (**2**) and ethanethiol (**3**), thereby

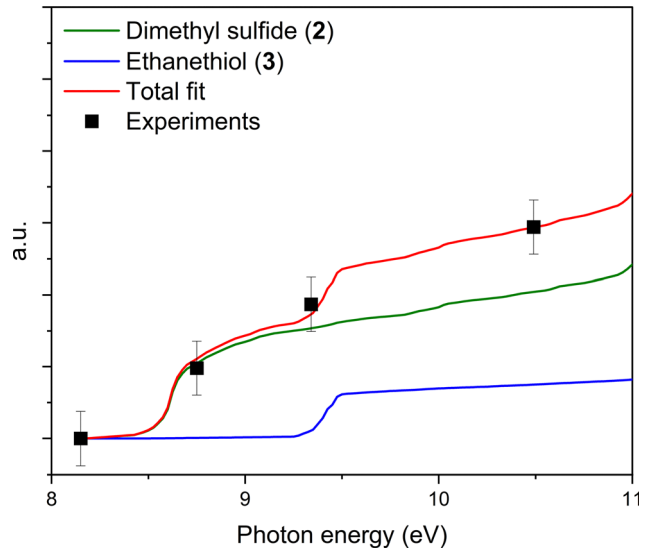

Fig. 8 Integrated signal counts at m/z = 62 subliming in the range from 109–151 K for C_2H_6S isomers for photoionization experiments at VUV energies; 8.17 eV, 8.75 eV, 9.34 eV and 10.49 eV (black) are compared to the individual photoionization efficiency (PIE) curves of dimethyl sulfide (**2**, green, obtained from Frost *et al.* photoelectron spectrum) and ethanethiol (**3**, blue, obtained from Ogata *et al.* photoelectron spectrum) and the total fit (red) of the PIE curves obtained by taking the sum of individual curves.

suggesting the formation of isomer **3** in these interstellar analog ices.

Potential mechanistical pathways

Having confirmed the formation of methanethiol (**1**), dimethyl sulfide (**2**) and its isomer ethanethiol (**3**) in irradiated CH_4–H_2S ices, we now focus on their potential formation pathways. Reaction pathways leading to the formation of **1**, **2**, and **3** in the astrophysically relevant icy conditions are investigated in Fig. 9 *via* reactions (1)–(13). Proxies for the effect of GCRs on the icy grains over a typical lifespan of cold molecular clouds in form of energetic electrons are exploited in these experiments.[37,38] These simulate secondary electron cascades generated by the GCR penetrating the ices. The energetic electrons deposit the energy that may also drive classically forbidden endoergic reactions in the ice. During the irradiation, electrons deposit doses up to 7.3 eV molecule^{-1} for methane and 15.6 eV molecule^{-1} for hydrogen sulfide that can easily break the C–H bonding in methane (CH_4; bond energy = 4.5 eV) and S–H bond of hydrogen sulfide (H_2S; bond energy = 3.9 eV) generating suprathermal hydrogen atoms.[49,54] These suprathermal hydrogen atoms are mobile since they bear excess kinetic energy to overcome the diffusion barrier.

Methane (CH_4) can decay upon interaction with energetic electrons through endoergic homolytic C–H bond cleavage forming suprathermal hydrogen atoms (H) and methyl (CH_3, X^2A'') radicals (reaction (1)); this process is endoergic by 432 kJ mol^{-1} (4.48 eV).[49,60] Methylene (CH_2, a^1A_1) radicals can be formed *via* reaction (2), endoergic by 458 kJ mol^{-1} (4.75 eV).[49,61,62]

$$CH_4 \rightarrow CH_3 + H \quad (1)$$

$$CH_4 \rightarrow CH_2 + H_2 \quad (2)$$

Endoergic (376 kJ mol^{-1} or 3.90 eV) homolytic bond cleavages of hydrogen sulfide (H_2S) can form sulfanyl (HS, $X^2\Pi$) and hydrogen (H) radicals. Likewise, this leads to sulfur in its first electronically excited state (S,^{1}D) and molecular hydrogen; this process is endoergic by 405 kJ mol^{-1} (4.20 eV) (reactions (3) and (4)).[61,63]

$$H_2S \rightarrow HS + H \quad (3)$$

$$H_2S \rightarrow S + H_2 \quad (4)$$

These formed radicals and atoms can undergo barrierless recombination or insertion to form first generation of irradiation products. Ethane (C_2H_6) can be formed by the combination of two methyl (CH_3) radicals[49,64,65] or *via* a methylene (CH_2) radical inserting into a C–H bond of methane[49,64–66] (Fig. 9: reactions (5) and (6)). A sulfanyl (HS) radical combining with a methyl (CH_3) radical can easily form methanethiol (CH_3SH) barrierlessly (Fig. 9: reaction (7)). Barrierless insertions of methylene (CH_2) into the S–H bonds of hydrogen sulfide (H_2S) and sulfur atoms (S(^{1}D)) insertion to C–H bonding in methane (CH_4) can also form methanethiol (Fig. 9: reactions (8) and (9)). Formation of ethane (C_2H_6) was identified on these CH_4–H_2S ices *via* multiple infrared absorption bands. The IE of ethane is 11.52 ± 0.04 eV,[45] higher than the maximum photon energy of 10.49 eV employed in this study; therefore, ethane cannot be ionized at 10.49 eV, whereas the formation methanethiol (**1**) was confirmed *via* PI-ReToF-MS.

Branching ratios can be investigated to distinguish which mechanisms are preferred in the formation of methanethiol (**1**). In the irradiated CH_4–D_2S ice, partially deuterated methanethiol (**1**) molecules are detected at m/z = 48 (CH_3SH), m/z = 49 (CH_3SD), and m/z = 50 (CH_2D_2S and $CH_3{}^{34}SH$). PI-ReToF-MS data collected with 10.49 eV photons for CH_3SH, CH_3SD and CH_2D_2S molecules in irradiated CH_4–D_2S ice formed *via* sulfur atom insertion, methyl (CH_3) plus sulfanyl (SH) radical combination, and methylene (CH_2) insertion into the S–D bond of deuterium sulfide (D_2S) are compared in the top panel of Fig. 10. Considering the 4.21% natural isotopic abundance of ^{34}S, signal expected for $CH_3{}^{34}SD$ (m/z = 51) based on CH_3SD (m/z = 49), and $CH_2D_2{}^{34}S$ (m/z = 52) based on CH_2D_2S (m/z = 50) were calculated. The projections for $CH_3{}^{34}SD$ (m/z = 51) and $CH_2D_2{}^{34}S$ (m/z = 52) were compared to signal observed at the respective mass channels m/z = 51 and m/z = 52 (Fig. 10: top). Observed branching ratios between the three reaction mechanisms, *i.e.* radical recombination, methylene or sulfur atom insertions, were calculated by integrating the signals observed for each molecule in the CH_4–D_2S ice. Radical combination of methyl and sulfanyl radicals contributed to 68 ± 2% of methanethiol (**1**) formation, while 26 ± 2% formed *via* CH_2 radical insertion and a 6 ± 1% *via* S(^{1}D) insertion to ethane molecules. Likewise, methanethiol (**1**) formation in the CD_4–H_2S ice is observed at m/z = 50 (CH_2D_2S), m/z = 51 (CD_3SH), and m/z = 52 (CD_3SD and $CH_2D_2{}^{34}S$) (Fig. 5E). Signal observed at m/z = 53 and m/z = 54 were compared with the expected signals of

CH_4 and H_2S ice

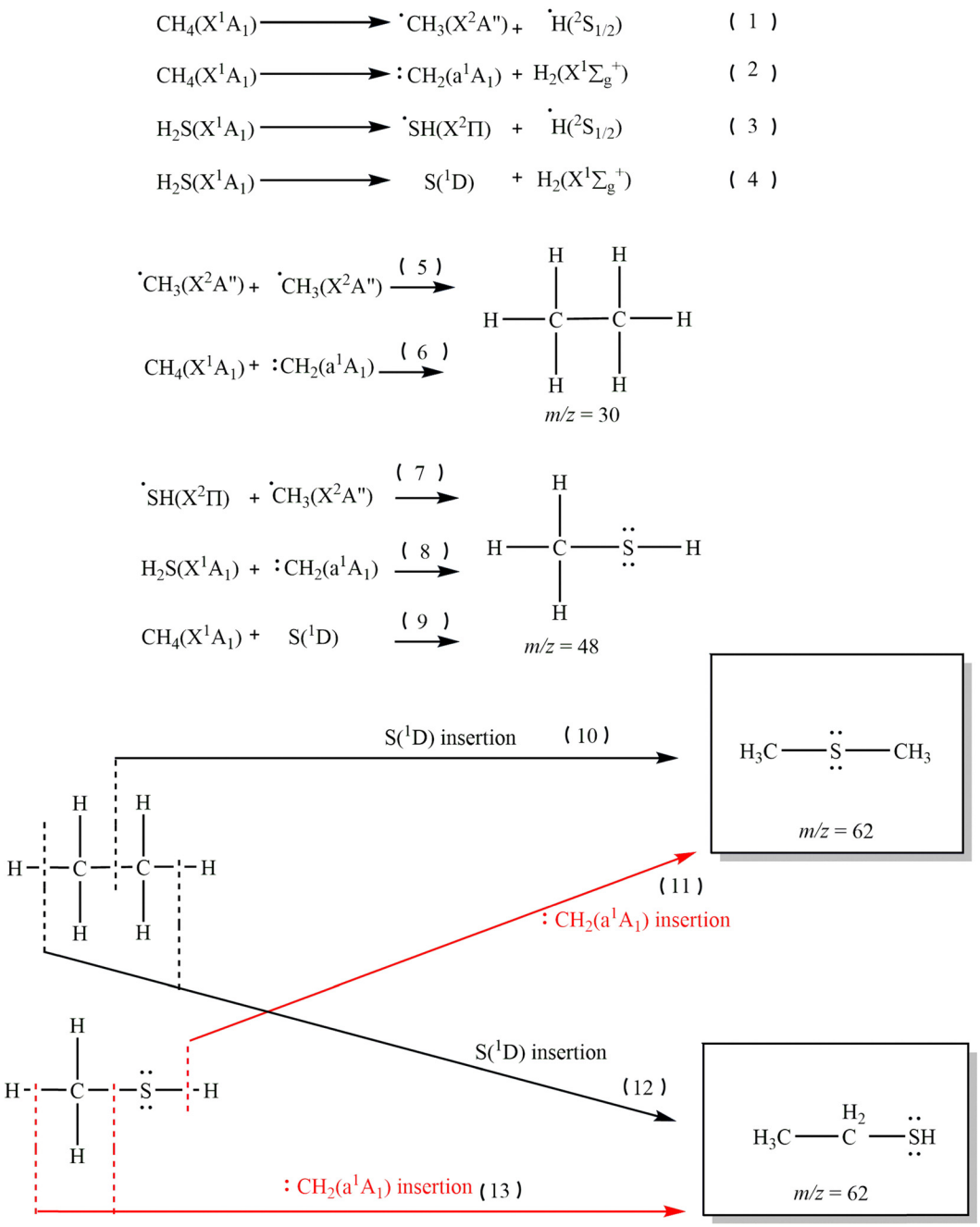

Fig. 9 Retrosynthetic formation pathways of dimethyl sulfide (**2**, CH_3SCH_3) and ethanethiol (**3**, C_2H_5SH) in the methane and hydrogen sulfide (CH_4–H_2S) ice.

$CD_3{}^{34}SH$ (m/z = 53) and $CD_3{}^{34}SD$ (m/z = 54) to confirm the assignments (Fig. 10: bottom). Note that the sublimation peak at 90 K is due to co-sublimation with H_2S. In the CD_4–H_2S ice, radical combination amounted to 70 ± 2% of methanethiol (**1**) formation, 20 ± 2% *via* CD_2 insertion to H_2S and only a 10 ± 2% *via* sulfur atom insertion to deuterated ethane. Branching ratios for **1** amongst the two deuterated ices are compared in Table 5.

Dimethyl sulfide (**2**) and ethanethiol (**3**) are second-generation irradiation products formed in these ices. Formation of isomer **2** can proceed either *via* S(^{1}D) insertion into the C–C bond of ethane or *via* methylene inserting into the S–H bond of methanethiol (Fig. 9: reactions (10) and (11)). Ethanethiol (**3**) is statistically more likely to be formed in these ices *via* S(^{1}D) insertion into any of the six C–H bonds of ethane and methylene radical insertions into the C–S or C–H bonds of methanethiol (Fig. 9: reactions (12) and (13)).

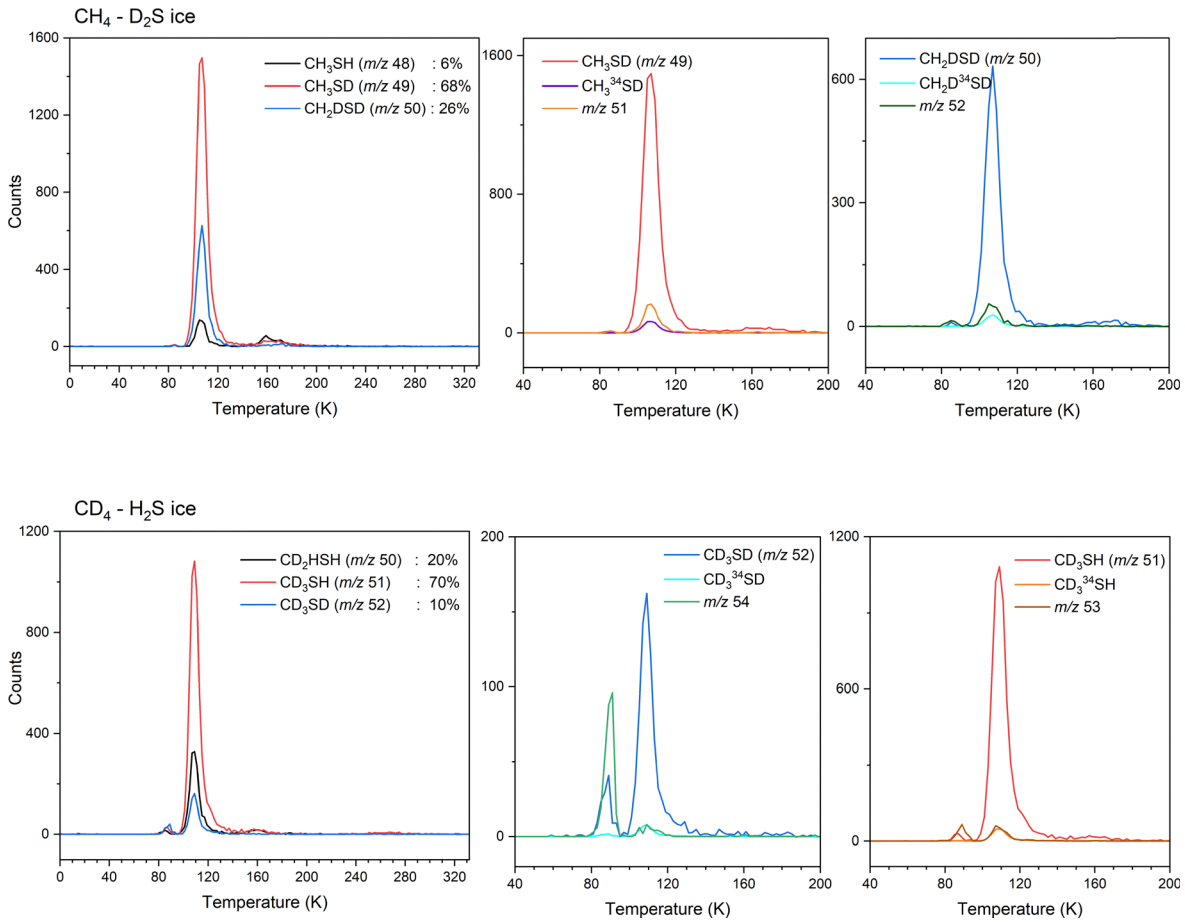

Fig. 10 TPD profiles for methanethiol (CH_3SH) in top: methane (CH_4) and deuterated hydrogen sulfate (D_2S) and bottom: deuterated methane (CD_4) and hydrogen sulfide (H_2S) irradiated ices. The percentages of each isotopologue observed are listed on each panel along with the mass-to-charge.

Table 5 Observed ratios of deuterated methanethiol isotopologues in each experiment and the proposed branching ratios for each of the three mechanisms in the irradiated methane and hydrogen sulfide ices

Observed m/z of methanethiol in CH_4 : H_2S ice	Observed m/z of methanethio in CH_4 : D_2S ice	Proposed formula in CH_4 : D_2S ice	Observed m/z of methanethiol in CD_4 : H_2S ice	Proposed formula in CD_4 : H_2S ice
m/z 48	m/z = 48 : 6 ± 1%	CH_3SH	m/z = 52 : 10 ± 2%	CD_3SD
	m/z = 49 : 68 ± 2%	CH_3SD	m/z = 51 : 70 ± 2%	CD_3SH
	m/z = 50 : 26 ± 2%	CH_2DSD	m/z = 50 : 20 ± 2%	CD_2HSH

In both partially deuterated ices of CH_4–D_2S (Fig. 6B) and CD_4–H_2S (Fig. 6C), methylene insertion to methanethiol route showed the highest signal intensities: $C_2H_4SD_2$ at m/z = 64 (Fig. 6B) and $C_2D_4H_2S$ at m/z = 66 (Fig. 6C).

In addition to **1** and **2**, sulfanes (H_2S_n: n = 2–11), and octasulfur (S_8)—which were identified forming on electron irradiated pure hydrogen sulfide ices[22]—were also observed in these methane–hydrogen sulfide ices, amongst the plethora of molecules subliming to the gas phase (Fig. S4–S7). Natural isotopic ratio between ^{32}S and ^{34}S was employed in demonstrating the signal corresponding to sulfanes ($H_2S_n^+$) ions in the mass channels shared with sulfur fragments ($^{32}S_n{}^{34}S^+$). Furthermore, ion signals corresponding to mass channels of CH_4S_n: n = 1–9, and $C_2H_6S_n$: n = 1–9 that can be either alkylsulfanes or alkylsulfur-ethers were also observed to be formed on these ices exposed to the high irradiation dose (Fig. S8).

Conclusions

Our results propose the abiotic formation of methanethiol (**1**), dimethyl sulfide (**2**) and ethanethiol (**3**) under interstellar conditions *via* a series of laboratory experiments using methane (CH_4) and hydrogen sulfide (H_2S) ices that simulate astrophysically relevant temperatures and pressures. The reaction pathways leading to **2** and **3** were investigated using isotopically labeled ices CH_4–D_2S and CD_4–H_2S with a low irradiation dose. Ethane (C_2H_6) and methanethiol (**1**, CH_3SH),

which are the first-generation irradiation products of crucial importance to the provided reaction mechanisms were also identified *via* infrared spectroscopy and photoionization reflectron time-of-flight mass spectrometry. Radical combination of methyl (CH_3) and sulfanyl (HS) radicals proved the major formation pathway towards methanethiol formation accounting for 68 ± 2% in CH_4–D_2S ice and 70 ± 2% in CD_4–H_2S ice.

Similar to the sulfanes and alkyl sulfanes forming in hydrogen sulfide (H_2S) and methane (CH_4) ices, the homologous series of phosphanes (P_2H_4 to P_8H_{10}) and methylphosphanes (CH_3PH_2 to $CH_3P_8H_9$) were reported forming in phosphine (PH_3) and methane (CH_4) ices.[41,67] But oxygen, which is isovalent to sulfur, was only found to form chains up to three atoms such as hydroxyperoxymethane (H_3COOOH), in extraterrestrial conditions.[68] The complex organosulfur molecules of $C_nH_mS_p$ (n = 0 to 4, m = 0 to 6, and p = 1, 2) in cometary coma of 67P/CG[19] may have been formed following mechanistic processes similar to such discussed here. Since these organosulfur molecules are feasible to form abiotically in interstellar or cometary ices, methanethiol or dimethyl sulfide cannot be simply interpreted as biomarkers for extraterrestrial life. Moreover, organosulfur molecules can be another possible sulfur sink for interstellar sulfur in ices that can be accounted towards the missing sulfur budget[69–71] in the interstellar medium.

Conflicts of interest

The authors declare no conflicting interests.

Data availability

Supplementary information (SI) is available. See DOI: https://doi.org/10.1039/d5cp04456a.

Essential data are provided in the main text. Additional data are available from the corresponding author upon reasonable request.

Acknowledgements

The authors would like to thank the US National Science Foundation (NSF) Division for Astronomy (NSF-AST 2403867) for support, W. M. Keck Foundation (R. I. K.) for financing the experimental setup, and the University of Hawai'i for providing Teaching Assistantships (A. H., M. M.).

References

1 C. Sagan, W. R. Thompson, R. Carlson, D. Gurnett and C. Hord, A search for life on Earth from the Galileo spacecraft, *Nature*, 1993, **365**, 715–721.
2 S. Seager, W. Bains and J. J. Petkowski, Toward a List of Molecules as Potential Biosignature Gases for the Search for Life on Exoplanets and Applications to Terrestrial Biochemistry, *Astrobiology*, 2016, **16**, 465–485.
3 C. B. Pilcher, Biosignatures of Early Earths, *Astrobiology*, 2003, **3**, 471–486.
4 J. P. Megonigal, M. E. Hines and P. T. Visscher, Anaerobic Metabolism: Linkages to Trace Gases and Aerobic Processes, *Treatise Geochem.*, 2003, **8–9**, 317–424.
5 S. Seager, W. Bains and R. Hu, Biosignature gases in H_2-dominated atmospheres on rocky exoplanets, *Astrophys. J.*, 2013, **777**, 95.
6 N. Madhusudhan, A. A. A. Piette and S. Constantinou, Habitability and Biosignatures of Hycean Worlds, *Astrophys. J.*, 2021, **918**, 1.
7 N. Madhusudhan, S. Constantinou, M. Holmberg, S. Sarkar, A. A. A. Piette and J. I. Moses, New Constraints on DMS and DMDS in the Atmosphere of K2-18 b from JWST MIRI, *Astrophys. J., Lett.*, 2025, **983**, L40.
8 C. S. Foden, S. Islam, C. Fernández-garcía, L. Maugeri, T. D. Sheppard and M. W. Powner, Prebiotic synthesis of cysteine peptides that catalyze peptide ligation in neutral water, *Science*, 2020, **370**, 865–869.
9 A. Manna and S. Pal, First Identification and Chemical Modeling of New Thiol (–SH) Bearing Molecule in the Interstellar Medium: Dithioformic Acid, *ACS Earth Space Chem.*, 2024, **8**, 2401–2410.
10 L. F. Rodríguez-Almeida, I. Jiménez-Serra, V. M. Rivilla, J. Martín-Pintado, S. Zeng, B. Tercero, P. de Vicente, L. Colzi, F. Rico-Villas, S. Martín and M. A. Requena-Torres, Thiols in the Interstellar Medium: First Detection of HC(O)SH and Confirmation of C_2H_5SH, *Astrophys. J., Lett.*, 2021, **912**, L11.
11 R. A. Linke, M. A. Frerking and P. Thaddeus, Interstellar methyl mercaptan, *Astrophys. J.*, 1979, **234**, L139.
12 L. Kolesniková, B. Tercero, J. Cernicharo, J. L. Alonso, A. M. Daly, B. P. Gordon and S. T. Shipman, Spectroscopic characterization and detection of ethyl mercaptan in orion, *Astrophys. J., Lett.*, 2014, **784**, 1–8.
13 E. Gibb, A. Nummelin, W. M. Irvine, D. C. B. Whittet and P. Bergman, Chemistry of the Organic-rich Hot Core G327.3–0.6, *Astrophys. J.*, 2000, **545**, 309–326.
14 H. A. Bunn, S. Spezzano, L. H. Coudert, J. Guillemin, Y. Lin, C. P. Endres, B. Billinghurst, O. Pirali, J. Jørgensen, V. Lattanzi and P. Caselli, Laboratory Rotational Spectroscopy Leads to the First Interstellar Detection of Singly Deuterated Methyl Mercaptan (CH_2DSH), *Astrophys. J., Lett.*, 2025, **980**, L13.
15 M. Sanz-Novo, V. M. Rivilla, C. P. Endres, V. Lattanzi, I. Jiménez-Serra, L. Colzi, S. Zeng, A. Megías, Á. López-Gallifa, A. Martínez-Henares, D. San Andrés, B. Tercero, P. de Vicente, S. Martín, M. A. Requena-Torres, P. Caselli and J. Martín-Pintado, On the Abiotic Origin of Dimethyl Sulfide: Discovery of Dimethyl Sulfide in the Interstellar Medium, *Astrophys. J., Lett.*, 2025, **980**, L37.
16 U. Calmonte, K. Altwegg, H. Balsiger, J. J. Berthelier, A. Bieler, G. Cessateur, F. Dhooghe, E. F. van Dishoeck, B. Fiethe, S. A. Fuselier, S. Gasc, T. I. Gombosi, M. Hässig, L. Le Roy, M. Rubin, T. Sémon, C.-Y. Tzou and S. F. Wampfler, Sulphur-bearing species in the coma of comet 67P/Churyumov–Gerasimenko, *Mon. Not. R. Astron. Soc.*, 2016, **462**, S253–S273.

17 L. Le Roy, K. Altwegg, H. Balsiger, J. J. Berthelier, A. Bieler, C. Briois, U. Calmonte, M. R. Combi, J. De Keyser, F. Dhooghe, B. Fiethe, S. A. Fuselier, S. Gasc, T. I. Gombosi, M. Hassig, A. Jackel, M. Rubin and C. Y. Tzou, Inventory of the volatiles on comet 67P/Churyumov–Gerasimenko from Rosetta/ROSINA, *Astron. Astrophys.*, 2015, **583**, A1.

18 N. Hänni, K. Altwegg, M. Combi, S. A. Fuselier, J. De Keyser, N. F. W. Ligterink, M. Rubin and S. F. Wampfler, Evidence for Abiotic Dimethyl Sulfide in Cometary Matter, *Astrophys. J.*, 2024, **976**, 74.

19 A. Mahjoub, K. Altwegg, M. J. Poston, M. Rubin, R. Hodyss, M. Choukroun, B. L. Ehlmann, N. Hänni, M. E. Brown, J. Blacksberg, J. M. Eiler and K. P. Hand, Complex organosulfur molecules on comet 67P: Evidence from the ROSINA measurements and insights from laboratory simulations, *Sci. Adv.*, 2023, eadh0394.

20 A. Mahjoub, M. J. Poston, J. Blacksberg, J. M. Eiler, M. E. Brown, B. L. Ehlmann, R. Hodyss, K. P. Hand, R. Carlson and M. Choukroun, Production of Sulfur Allotropes in Electron Irradiated Jupiter Trojans Ice Analogs, *Astrophys. J.*, 2017, **846**, 148.

21 Y. J. Chen, K. J. Juang, M. Nuevo, A. Jiménez-Escobar, G. M. Muñoz Caro, J. M. Qiu, C. C. Chu, T. S. Yih, C. Y. R. Wu, H. S. Fung and W. H. Ip, Formation of s-bearing species by VUV/EUV irradiation of H_2S-containing ice mixtures: Photon energy and carbon source effects, *Astrophys. J.*, 2024, 80.

22 A. Herath, M. McAnally, A. M. Turner, J. Wang, J. H. Marks, R. C. Fortenberry, J. C. Garcia-Alvarez, S. Gozem and R. I. Kaiser, Missing interstellar sulfur in inventories of polysulfanes and molecular octasulfur crowns, *Nat. Commun.*, 2025, **16**, 1–13.

23 G. Strazzulla, M. Garozzo and O. Gomis, The origin of sulfur-bearing species on the surfaces of icy satellites, *Adv. Space Res.*, 2009, **43**, 1442–1445.

24 S. Cazaux, H. Carrascosa, G. M. Muñoz Caro, P. Caselli, A. Fuente, D. Navarro-Almaida and P. Riviére-Marichalar, Photoprocessing of H_2S on dust grains, *Astron. Astrophys.*, 2022, **657**, A100.

25 A. Jiménez-Escobar, G. M. Muñoz Caro and Y.-J. Chen, Sulphur depletion in dense clouds and circumstellar regions. Organic products made from UV photoprocessing of realistic ice analogs containing H_2S, *Mon. Not. R. Astron. Soc.*, 2014, **443**, 343–354.

26 J. Wang, J. H. Marks, L. B. Tuli, A. M. Mebel, V. N. Azyazov and R. I. Kaiser, Formation of Thioformic Acid (HCOSH)—The Simplest Thioacid—in Interstellar Ice Analogues, *J. Phys. Chem. A*, 2022, **126**, 9699–9708.

27 M. H. Moore, R. L. Hudson and R. W. Carlson, The radiolysis of SO_2 and H_2S in water ice: Implications for the icy jovian satellites, *Icarus*, 2007, **189**, 409–423.

28 M. Garozzo, D. Fulvio, Z. Kanuchova, M. E. Palumbo and G. Strazzulla, The fate of S-bearing species after ion irradiation of interstellar icy grain mantles, *Astron. Astrophys.*, 2010, **509**, 1–9.

29 J. C. Santos, J. Enrique-Romero, T. Lamberts, H. Linnartz and K.-J. Chuang, Formation of S-Bearing Complex Organic Molecules in Interstellar Clouds *via* Ice Reactions with C_2H_2, HS, and Atomic H, *ACS Earth Space Chem.*, 2024, **8**, 1646–1660.

30 M. McAnally, J. Bocková, A. Herath, A. M. Turner, C. Meinert and R. I. Kaiser, Abiotic formation of alkylsulfonic acids in interstellar analog ices and implications for their detection on Ryugu, *Nat. Commun.*, 2024, **15**, 4409.

31 A. Ruf, A. Bouquet, P. Boduch, P. Schmitt-Kopplin, V. Vinogradoff, F. Duvernay, R. G. Urso, R. Brunetto, L. Le Sergeant d'Hendecourt, O. Mousis and G. Danger, Organosulfur Compounds Formed by Sulfur Ion Bombardment of Astrophysical Ice Analogs: Implications for Moons, Comets, and Kuiper Belt Objects, *Astrophys. J., Lett.*, 2019, **885**, 1–31.

32 A. Bouquet, C. A. P. da Costa, P. Boduch, H. Rothard, A. Domaracka, G. Danger, I. Schmitz, C. Afonso, P. Schmitt-Kopplin, V. Hue, T. A. Nordheim, A. Ruf, F. Duvernay, M. Napoleoni, N. Khawaja, F. Postberg, T. Javelle, O. Mousis and L. I. Tenelanda Osorio, Sulfur Implantation into Water Ice with Propane: Implications for Organic Chemistry on the Surface of Europa, *Planet. Sci. J.*, 2024, **5**, 102.

33 H. Carrascosa, G. M. Muñoz Caro, R. Martín-Doménech, S. Cazaux, Y.-J. Chen and A. Fuente, Formation and desorption of sulphur chains ($H2S_x$ and S_x) in cometary ice: effects of ice composition and temperature, *Mon. Not. R. Astron. Soc.*, 2024, **533**, 967–978.

34 N. W. Reed, R. L. Shearer, S. E. McGlynn, B. A. Wing, M. A. Tolbert and E. C. Browne, Abiotic Production of Dimethyl Sulfide, Carbonyl Sulfide, and Other Organosulfur Gases via Photochemistry: Implications for Biosignatures and Metabolic Potential, *Astrophys. J., Lett.*, 2024, **973**, L38.

35 R. I. Kaiser, Experimental Investigation on the Formation of Carbon-Bearing Molecules in the Interstellar Medium via Neutral–Neutral Reactions, *Chem. Rev.*, 2002, **102**, 1309–1358.

36 C. J. Bennett, Y. Osamura, M. D. Lebar and R. I. Kaiser, Laboratory Studies on the Formation of Three C_2H_4O Isomers—Acetaldehyde (CH_3CHO), Ethylene Oxide (c-C_2H_4O), and Vinyl Alcohol (CH_2CHOH)—in Interstellar and Cometary Ices, *Astrophys. J.*, 2005, **634**, 698–711.

37 A. G. Yeghikyan, Irradiation of dust in molecular clouds. II. Doses produced by cosmic rays, *Astrophysics*, 2011, **54**, 87–99.

38 A. M. Turner and R. I. Kaiser, Exploiting Photoionization Reflectron Time-of-Flight Mass Spectrometry to Explore Molecular Mass Growth Processes to Complex Organic Molecules in Interstellar and Solar System Ice Analogs, *Acc. Chem. Res.*, 2020, **53**, 2791–2805.

39 M. J. Abplanalp, A. Borsuk, B. M. Jones and R. I. Kaiser, On the formation and isomer specific detection of propenal (C_2H_3CHO) and cyclopropanone (c-C_3H_4O) in interstellar model ices—A combined FTIR and reflectron time-of-flight mass spectroscopic study, *Astrophys. J.*, 2015, **814**, 45.

40 R. L. Hudson and P. A. Gerakines, Infrared Spectra and Interstellar Sulfur: New Laboratory Results for H 2 S and Four Malodorous Thiol Ices, *Astrophys. J.*, 2018, **867**, 138.

41 A. M. Turner, M. J. Abplanalp, S. Y. Chen, Y. T. Chen, A. H. H. Chang and R. I. Kaiser, A photoionization mass spectroscopic study on the formation of phosphanes in low temperature phosphine ices, *Phys. Chem. Chem. Phys.*, 2015, **17**, 27281–27291.
42 A. M. Turner, M. J. Abplanalp, T. J. Blair, R. Dayuha and R. I. Kaiser, An Infrared Spectroscopic Study Toward the Formation of Alkylphosphonic Acids and Their Precursors in Extraterrestrial Environments, *Astrophys. J., Suppl. Ser.*, 2018, **234**, 6.
43 D. Drouin, A. R. Couture, D. Joly, X. Tastet, V. Aimez and R. Gauvin, CASINO V2.42—A Fast and Easy-to-use Modeling Tool for Scanning Electron Microscopy and Microanalysis Users, *Scanning*, 2007, **29**, 92–101.
44 J. Wang, J. H. Marks, A. M. Turner, A. A. Nikolayev, V. Azyazov, A. M. Mebel and R. I. Kaiser, Mechanistical study on the formation of hydroxyacetone (CH_3COCH_2OH), methyl acetate (CH_3COOCH_3), and 3-hydroxypropanal ($HCOCH_2CH_2OH$) along with their enol tautomers (prop-1-ene-1,2-diol ($CH_3C(OH)CHOH$), prop-2-ene-1,2-diol ($CH_2C(OH)CH_2OH$), *Phys. Chem. Chem. Phys.*, 2023, **25**, 936–953.
45 S. G. Lias, in *NIST Chemistry WebBook, NIST Standard Reference Database Number 69*, ed. P. J. Linstrom and W. G. Mallard, National Institute of Standards and Technology, Gaithersburg MD, 20899, 2024.
46 J. H. Marks, X. Bai, A. A. Nikolayev, Q. Gong, M. McAnally, J. Wang, Y. Pan, R. C. Fortenberry, A. M. Mebel, T. Yang and R. I. Kaiser, Methanetetrol and the final frontier in ortho acids, *Nat. Commun.*, 2025, **16**, 6468.
47 K. Fathe, J. S. Holt, S. P. Oxley and C. J. Pursell, Infrared spectroscopy of solid hydrogen sulfide and deuterium sulfide, *J. Phys. Chem. A*, 2006, **110**, 10793–10798.
48 F. Salama, L. J. Allamandola, F. C. Witteborn, D. P. Cruikshank, S. A. Sandford and J. D. Bregman, The 2.5-5.0 μm spectra of Io: evidence for H_2S and H_2O frozen in SO_2, *Form. Stars planets, Evol. Sol. Syst. Proc. 24th ESLAB Symp. Friedrichshafen*, 1990, vol. 1990, 2, pp. 203–208.
49 C. J. Bennett, C. S. Jamieson, Y. Osamura and R. I. Kaiser, Laboratory Studies on the Irradiation of Methane in Interstellar, Cometary, and Solar System Ices, *Astrophys. J.*, 2006, **653**, 792–811.
50 N. Zengin and P. A. Giguère, Infrared spectrum of crystalline H_2S_2, *Can. J. Chem.*, 1959, **37**, 632–634.
51 S. Maity, Y. S. Kim, R. I. Kaiser, H. M. Lin, B. J. Sun and A. H. H. Chang, On the detection of higher order carbon sulfides (CS_x; x = 4–6) in low temperature carbon disulfide ices, *Chem. Phys. Lett.*, 2013, **577**, 42–47.
52 G. Socrates, *Infrared and Raman Characteristic Group Frequencies*, 3rd edn, 2004, vol. 5.
53 A. K. Eckhardt, A. Bergantini, S. K. Singh, P. R. Schreiner and R. I. Kaiser, Formation of Glyoxylic Acid in Interstellar Ices: A Key Entry Point for Prebiotic Chemistry, *Angew. Chem., Int. Ed.*, 2019, **58**, 5663–5667.
54 C. Zhu, S. Góbi, M. J. Abplanalp, R. Frigge, J. J. Gillis-Davis and R. I. Kaiser, Space Weathering-Induced Formation of Hydrogen Sulfide (H_2S) and Hydrogen Disulfide (H_2S_2) in the Murchison Meteorite, *J. Geophys. Res.:Planets*, 2019, **124**, 2772–2779.
55 E. A. Walters and N. C. Blais, Molecular beam photoionization and fragmentation of D_2S, $(H_2S)_2$, $(D_2S)_2$, and $H_2S{\cdot}H_2O$, *J. Chem. Phys.*, 1984, **3501**, 20–22.
56 J. Berkowitz, J. P. Greene, H. Cho and B. Ruscić, The ionization potentials of CH_4 and CD_4, *J. Chem. Phys.*, 1987, **674**, 22–25.
57 C. L. Liao and C. Y. Ng, Molecular beam photoionization study of S_2, *J. Chem. Phys.*, 1986, **84**, 778–782.
58 D. Frost, F. Herring, A. Katrib, C. Mcdowell and R. A. N. Mclean, Photoelectron spectra of CH_3SH, $(CH_3)_2S$, C_6H_5SH, and $C_6H_5CH_2SH$; the bonding between sulfur and carbon, *J. Phys. Chem.*, 1972, **76**, 1030–1034.
59 H. Ogata, H. Onizuka, Y. Nihei and H. Kamada, The Photoelectron Spectra of Alcohols, Mercaptans and Amines, *Bull. Chem. Soc. Jpn.*, 1973, **46**, 3036–3040.
60 NIST chemistry WebBook, *Choice Rev. Online*, 2006, vol. 43, p. 43Sup-0293.
61 B. Ruscic, R. E. Pinzon, M. L. Morton, G. von Laszevski, S. J. Bittner, S. G. Nijsure, K. A. Amin, M. Minkoff and A. F. Wagner, Introduction to Active Thermochemical Tables: Several "Key" Enthalpies of Formation Revisited, *J. Phys. Chem. A*, 2004, **108**, 9979–9997.
62 B. Ruscic and D. H. Bross, Accurate and reliable thermochemistry by data analysis of complex thermochemical networks using Active Thermochemical Tables: the case of glycine thermochemistry, *Faraday Discuss.*, 2025, **256**, 345–372.
63 J. Zhou, Y. Zhao, C. S. Hansen, J. Yang, Y. Chang, Y. Yu, G. Cheng, Z. Chen, Z. He, S. Yu, H. Ding, W. Zhang, G. Wu, D. Dai, C. M. Western, M. N. R. Ashfold, K. Yuan and X. Yang, Ultraviolet photolysis of H_2S and its implications for SH radical production in the interstellar medium, *Nat. Commun.*, 2020, **11**, 1547.
64 M. J. Abplanalp, B. M. Jones and R. I. Kaiser, Untangling the methane chemistry in interstellar and solar system ices toward ionizing radiation: a combined infrared and reflectron time-of-flight analysis, *Phys. Chem. Chem. Phys.*, 2018, **20**, 5435–5468.
65 C. Zhu, A. M. Turner, M. J. Abplanalp and R. I. Kaiser, Formation and High-order Carboxylic Acids (RCOOH) in Interstellar Analogous Ices of Carbon Dioxide (CO_2) and Methane(CH_4), *Astrophys. J., Suppl. Ser.*, 2018, **234**, 15.
66 R. I. Kaiser and K. Roessler, Theoretical and Laboratory Studies on the Interaction of Cosmic-Ray Particles with Interstellar Ices. III. Suprathermal Chemistry–Induced Formation of Hydrocarbon Molecules in Solid Methane (CH_4), Ethylene (C_2H_4), and Acetylene (C_2H_2), *Astrophys. J.*, 1998, **503**, 959–975.
67 A. M. Turner, M. J. Abplanalp and R. I. Kaiser, Probing the carbon–phosphorous bond coupling in low-temperature phosphine (PH_3)–methane (CH_4) interstellar ice analogues, *Astrophys. J.*, 2016, **819**, 97.
68 J. H. Marks, X. Bai, A. A. Nikolayev, Q. Gong, C. Zhu, N. F. Kleimeier, A. M. Turner, S. K. Singh, J. Wang, J. Yang,

Y. Pan, T. Yang, A. M. Mebel and R. I. Kaiser, Methanetriol—Formation of an Impossible Molecule, *J. Am. Chem. Soc.*, 2024, **146**, 12174–12184.
69 S. S. Prasad and W. T. Huntress, JR, Sulfur chemistry in dense interstellar clouds, *Astrophys. J.*, 1982, **260**, 590.
70 D. P. Ruffle, T. W. Hartquist, P. Caselli and D. A. Williams, The sulphur depletion problem, *Mon. Not. R. Astron. Soc.*, 1999, **306**, 691–695.
71 J. C. Laas and P. Caselli, Modeling sulfur depletion in interstellar clouds, *Astron. Astrophys.*, 2019, A108.
72 J. He, K. Gao, G. Vidali, C. J. Bennett and R. I. Kaiser, Formation of molecular hydrogen from methane ice, *Astrophys. J.*, 2010, **721**, 1656–1662.
73 S. Maity and R. I. Kaiser, Electron irradiation of carbon disulfide-oxygen ices: Toward the formation of sulfur-bearing molecules in interstellar ices, *Astrophys. J.*, 2013, 184.